



Michigan Technological University  
*Create the Future* Digital Commons @ Michigan Tech

---

Dissertations, Master's Theses and Master's  
Reports - Open

Dissertations, Master's Theses and Master's  
Reports

---

2011

## Comparisons between OMI SO<sub>2</sub> data and ground-based SO<sub>2</sub> measurements at Turrialba volcano

Anieri M. Morales Rivera  
*Michigan Technological University*

Follow this and additional works at: <https://digitalcommons.mtu.edu/etds>

 Part of the [Geology Commons](#)


Copyright 2011 Anieri M. Morales Rivera

---

### Recommended Citation

Morales Rivera, Anieri M., "Comparisons between OMI SO<sub>2</sub> data and ground-based SO<sub>2</sub> measurements at Turrialba volcano ", Master's Thesis, Michigan Technological University, 2011.  
<https://doi.org/10.37099/mtu.dc.etds/334>

Follow this and additional works at: <https://digitalcommons.mtu.edu/etds>

 Part of the [Geology Commons](#)

COMPARISONS BETWEEN OMI SO<sub>2</sub> DATA AND GROUND-BASED SO<sub>2</sub>  
MEASUREMENTS AT TURRIALBA VOLCANO

By

Anieri M. Morales Rivera

A THESIS

Submitted in partial fulfillment of the requirements for the degree of

MASTER OF SCIENCE

(Geology)

MICHIGAN TECHNOLOGICAL UNIVERSITY

2011

© 2011 Anieri M. Morales Rivera

This thesis, “Comparisons between OMI SO<sub>2</sub> data and ground-based SO<sub>2</sub> measurements at Turrialba volcano,” is hereby approved in partial fulfillment of the requirements for the Degree of MASTER OF SCIENCE IN GEOLOGY.

Department of Geological and Mining Engineering and Sciences

Signatures:

Thesis Advisor \_\_\_\_\_  
Dr. Simon A. Carn

Committee Member \_\_\_\_\_  
Dr. Louisa J. Kramer

Committee Member \_\_\_\_\_  
Dr. Ann L. Maclean

Committee Member \_\_\_\_\_  
Dr. Lizzette A. Rodríguez

Department Chair \_\_\_\_\_  
Dr. Wayne D. Pennington

Date \_\_\_\_\_

# Table of Contents

List of Figures .....	v
List of Tables .....	vii
Abstract .....	viii
Acknowledgements.....	ix
1. Introduction.....	1
1.1 Geological Setting of the Study Area .....	7
1.1.1 Tectonic Setting .....	8
1.1.2 Morphostructural Features .....	10
1.1.3 Stratigraphic Record and Eruptive History .....	10
1.2 Previous Work on Turrialba.....	13
2. The Ozone Monitoring Instrument: Comparison of SO <sub>2</sub> mass calculations .....	15
2.1 The Ozone Monitoring Instrument .....	15
2.2 OMI Data Analysis .....	16
2.2.1 Band Residual Index .....	17
2.2.2 Normalized Cloud-mass.....	19
2.2.3 SO <sub>2</sub> Emission Rates from Cumulative Plots .....	21
2.3 Results and Discussion .....	23
2.3.1 Band Residual Index vs. Normalized Cloud-mass.....	23
2.3.2 OMI Cumulative Plot Technique.....	25
3. Comparisons between OMI SO <sub>2</sub> Data and Mini-DOAS measurements at Turrialba volcano...	32
3.1 Mini-DOAS Data Collection .....	32
3.1.1 MTU Resonance Mini-DOAS .....	32
3.1.2 NOVAC Version I Mini-DOAS .....	34
3.2 Mini-DOAS Data Analysis.....	34
3.2.1 MTU Resonance Mini-DOAS .....	34
3.2.2 NOVAC Mini-DOAS .....	37
3.3 OMI Data Analysis .....	37
3.3.1 MODIS Smoke Estimation Technique .....	37
3.3.2 OMI SO <sub>2</sub> Lifetime Technique.....	39



3.3.3 OMI SO <sub>2</sub> Transects Technique .....	41
3.4 Comparisons between OMI and Mini-DOAS .....	45
3.4.1 MODIS Smoke Estimation Technique .....	45
3.4.2 OMI SO <sub>2</sub> Lifetime Technique .....	47
3.4.3 OMI SO <sub>2</sub> Transects Technique .....	49
4. Conclusions .....	56
4.1 Future Work .....	57
5. References .....	59
6. Appendix .....	64
A: Steps and parameters used to obtain data from NOAA's READY web-based system .....	64
B: OMI monthly average SO <sub>2</sub> plots .....	66
C: Processed NOVAC data .....	67
D: MODIS smoke estimation technique .....	73
E: SO <sub>2</sub> transects from gridded OMI plots .....	76
F: Copyright for Figure 12 (Personal communication through e-mail) .....	88
G: Copyright for Appendix C (Personal communication through e-mail in Spanish) .....	89

## List of Figures

Figure 1: Location of Turrialba volcano in Costa Rica .....	9
Figure 2: View of Turrialba volcano and its plume (Left); and view of the West and Central craters at the summit (Right).....	9
Figure 3: High resolution SO <sub>2</sub> absorption cross-section from 310-315 nm. ....	18
Figure 4: Example of volcanic SO <sub>2</sub> pixel selection for an OMI daily image using the BRI technique. ....	19
Figure 5: Example of a daily OMI image of Costa Rica with the satellite almost at nadir. ....	20
Figure 6: Example of OMI monthly SO <sub>2</sub> average plot for July, 2010. ....	23
Figure 7: Turrialba NCM and BRI SO <sub>2</sub> mass time series plot for the year 2010.....	26
Figure 8: BRI SO <sub>2</sub> masses plotted against the NCM SO <sub>2</sub> masses for the year 2010 .....	27
Figure 9: BRI SO <sub>2</sub> masses plotted against the NCM SO <sub>2</sub> masses for the 2010 dry season .....	28
Figure 10: Cumulative SO <sub>2</sub> mass for Turrialba volcano during the year 2010. ....	30
Figure 11: Mini-DOAS system components (Left); and an example of the stationary measurement strategy with red lines representing the scanning under Turrialba's plume (Right) .....	33
Figure 12: Methods to determine the plume width when nearly above (A), and when directly above (B).....	35
Figure 13: Example of a daily OMI SO <sub>2</sub> image where the black dashed line represents the volcanic plume trajectory with a constant wind direction.....	40
Figure 14: Example of a daily OMI SO <sub>2</sub> image where the black dashed line represents the volcanic plume trajectory with a variable wind direction. ....	41
Figure 15 A: April 23, 2010 OMI SO <sub>2</sub> map used for SO <sub>2</sub> emission rate estimation using the plume transect technique.....	42
Figure 15 B: May 18, and June 10, 2010 OMI SO <sub>2</sub> maps used for SO <sub>2</sub> emission rate estimation using the plume transect technique .....	43
Figure 15 C: July 23, 2010, and January 28, 2011 OMI SO <sub>2</sub> maps used for SO <sub>2</sub> emission rate estimation using the plume transect technique.....	44
Figure 16: Comparisons between OMI data and Mini DOAS measurements under varying wind conditions .....	49
Figure 17: OMI SO <sub>2</sub> fluxes measured from plume transects compared to SO <sub>2</sub> fluxes obtained by the Mini-DOAS on April 23, 2010. ....	51
Figure 18: OMI SO <sub>2</sub> fluxes measured from plume transects compared to SO <sub>2</sub> fluxes obtained by the Mini-DOAS on May 18, 2010. ....	52

Figure 19: OMI SO <sub>2</sub> fluxes measured from plume transects compared to SO <sub>2</sub> fluxes obtained by the Mini-DOAS on June 10, 2010 .....	53
Figure 20: July 23, 2010 OMI image over the Aqua satellite image .....	55
Figure 21: OMI monthly average SO <sub>2</sub> plots for Costa Rica and Nicaragua during 2010 .....	66
Figure 22 A: Pixels selected for OMI analysis using the MODIS smoke estimation technique for April 28, and May 18, 2010. ....	73
Figure 22 B: Pixels selected for OMI analysis using the MODIS smoke estimation technique for May 30, and June 10, 2010. ....	74
Figure 22 C: Pixels selected for OMI analysis using the MODIS smoke estimation technique for August 13, 2010. ....	75

## List of Tables

Table 1: Stratigraphic record at Turrialba volcano .....	11
Table 2: Eruptive history of Turrialba volcano.....	12
Table 3: Maximum volcanic SO <sub>2</sub> lifetime per month and OMI cumulative SO <sub>2</sub> emissions for Turrialba during the year 2010.....	31
Table 4: Available data and parameters used during the mini-DOAS field deployment.....	33
Table 5: Time ranges per day for analyzed data from the NOVAC database.....	34
Table 6: SO <sub>2</sub> fluxes obtained during mini-DOAS field deployment at Turrialba volcano .....	36
Table 7: SO <sub>2</sub> fluxes obtained from OMI using the MODIS Smoke Emission Technique, and by averaging the results from the NOVAC Project Database.....	46
Table 8: Turrialba's volcanic SO <sub>2</sub> lifetime and fluxes under constant wind direction .....	48
Table 9: Turrialba's volcanic SO <sub>2</sub> lifetime and fluxes under varying wind directions.....	49
Table 10: SO <sub>2</sub> fluxes obtained by the Mini-DOAS and OMI transects on 4/23/2010 .....	51
Table 11: SO <sub>2</sub> fluxes obtained by the Mini-DOAS and OMI transects during 5/18/2010.....	52
Table 12: SO <sub>2</sub> fluxes obtained by the Mini-DOAS and OMI transects during 6/10/2010.....	53
Table 13: SO <sub>2</sub> fluxes obtained by the Mini-DOAS and OMI transects on 7/23/2010 .....	55
Table 14: SO <sub>2</sub> fluxes obtained by the Mini-DOAS and OMI transects during 1/28/2011.....	55
Table 15: NOVAC SO <sub>2</sub> fluxes (Galle et al., 2010), processed and provided by Vladimir Conde (personal communication, See Appendix G) .....	67

## Abstract

Turrialba is one of the largest and most active stratovolcanoes in the Central Cordillera of Costa Rica and an excellent target for validation of satellite data using ground based measurements due to its high elevation, relative ease of access, and persistent elevated SO<sub>2</sub> degassing. The Ozone Monitoring Instrument (OMI) aboard the Aura satellite makes daily global observations of atmospheric trace gases and it is used in this investigation to obtain volcanic SO<sub>2</sub> retrievals in the Turrialba volcanic plume. We present and evaluate the relative accuracy of two OMI SO<sub>2</sub> data analysis procedures, the automatic Band Residual Index (BRI) technique and the manual Normalized Cloud-mass (NCM) method. We find a linear correlation and good quantitative agreement between SO<sub>2</sub> burdens derived from the BRI and NCM techniques, with an improved correlation when wet season data are excluded. We also present the first comparisons between volcanic SO<sub>2</sub> emission rates obtained from ground-based mini-DOAS measurements at Turrialba and three new OMI SO<sub>2</sub> data analysis techniques: the MODIS smoke estimation, OMI SO<sub>2</sub> lifetime, and OMI SO<sub>2</sub> transect techniques. A robust validation of OMI SO<sub>2</sub> retrievals was made, with both qualitative and quantitative agreements under specific atmospheric conditions, proving the utility of satellite measurements for estimating accurate SO<sub>2</sub> emission rates and monitoring passively degassing volcanoes.

## **Acknowledgements**

I would like to thank my advisor Simon Carn for his mentoring and supervision throughout the project, for the detailed reviews and constructive comments on the manuscript. Lizzette Rodríguez, Ann Maclean and Louisa Kramer for their support, suggestions, and being part of my committee. John Gierke for his advising throughout my graduate studies. Carlos Ramírez for our many attempts to collect data on the field, for his advising and support. Robert Mani for his help with the Resonance Mini-DOAS and software. The University of Costa Rica (UCR), Red Sismológica Nacional (RSN), and Instituto Costarricense de Electricidad (ICE): Gerardo Soto, Mauricio Mora, Raúl Mora, Gino González, Carlos Redondo, Jose Arias (Chico), and Sergio Guillén for their support and assistance during field deployment in Costa Rica. Cristina López and Cherrymar Reyes from the University of Puerto Rico at Mayagüez (UPRM) for field assistance. Vladimir Conde for providing the processed NOVAC data. The King Chavez Parks Future Faculty Fellowship for funding my graduate studies. The National Science Foundation Partnership for International Research and Education (NSF PIRE 0530109) for funding my project. Friends and family for your support.

# 1. Introduction

Sulfur dioxide (SO<sub>2</sub>) gas is a dangerous atmospheric pollutant that is emitted by both anthropogenic and natural sources. Volcanoes emit SO<sub>2</sub> during both eruptive and non-eruptive (or ‘passive’) activity, having a typical lifetime in the lower troposphere of approximately one day before being deposited or oxidized to sulfate (Stevenson et al., 2003). Sulfates are a major component of atmospheric aerosol particles and have a tropospheric lifetime of approximately 5 days (Delmelle, 2003). Volcanic emissions of SO<sub>2</sub> and other soluble gases (e.g., hydrogen chloride, HCl) generate highly acidic clouds and acid rain that can negatively impact surrounding ecosystems and infrastructure, and result in economic losses (Delmelle et al., 2002). Sulfate aerosol also scatters shortwave solar radiation, cooling the atmosphere below (Charlson et al., 1992), and absorbs longwave (infrared, IR) radiation, causing local warming. Health hazards associated with exposure to SO<sub>2</sub> are also well documented, and include irritation of the skin, eyes, nose, and throat, and serious effects on the respiratory system (Hansell and Oppenheimer, 2004). Passively degassing volcanoes can have significant impacts on tropospheric chemistry, and therefore impact the climate and environment on local and regional scales.

Other than understanding the effects on atmospheric chemistry and the environment, monitoring volcanic SO<sub>2</sub> is of extreme importance because changes in SO<sub>2</sub> emission rates provide information on magmatic processes occurring in volcanic systems and can be a precursor of volcanic eruptions (Casadevall et al., 1981; Edmonds et al., 2003b; Watson et al., 2000; Young et al., 1998). SO<sub>2</sub> emission rates have also been used in conjunction with petrological data to derive estimations of degassed magma volumes

(Allard et al., 1994). Silicate melt inclusions can maintain their original dissolved volatile concentrations, and thus can give us the concentration of sulfur from pre-erupted magmas (Shinohara, 2008). Information such as the density of the erupted magma along with the sulfur concentration obtained from both melt inclusions and SO<sub>2</sub> emission rates for a given amount of time can be used to estimate the minimum volume of the magma. This information is useful to assess constraints upon the feeding system, magma dynamics, and volatile transfer from the earth's interior (Allard, 1997).

The low atmospheric background concentration of SO<sub>2</sub> along with its strong absorption features in the ultraviolet (UV) region of the electromagnetic spectrum make this gas ideal for spectroscopic measurements using scattered sunlight (Campion et al., 2010). The ground-based correlation spectrometer (COSPEC) instrument was developed for pollution monitoring and, subsequently used for volcanic SO<sub>2</sub> surveillance in the 1960's and 1970's (Moffat and Millan, 1971; Stoiber and Jepsen, 1973). The COSPEC is used to obtain vertical or slant column measurements of SO<sub>2</sub> by making traverses beneath the volcanic plume either manually via scanning from a fixed position or, more typically, on a moving platform (William-Jones et al., 2008). Even though it has played an important role in volcano monitoring and during many volcanic crises and eruptions (e.g. Kilauea, Mount St. Helens, Pinatubo, Soufrière Hills), it is currently being replaced by less expensive and more compact UV spectrometers. One example is the Miniature Differential Optical Absorption Spectrometer or 'Mini-DOAS', whose newest version consists of a scanning instrument that scans a vertical plane as nearly perpendicular to the plume direction (Galle et al., 2003).



Satellite-based instruments operating in the UV region have been used for monitoring volcanic SO<sub>2</sub> since the detection of the plume from the 1982 eruption of El Chichón volcano (Mexico) by the Total Ozone Mapping Spectrometer (TOMS) (Krueger, 1983). The TOMS record of volcanic SO<sub>2</sub> emissions extends from 1978 to 2005 (Bluth et al., 1994; Carn et al., 2003). Since 2004, a more advanced UV sensor, the Ozone Monitoring Instrument (OMI), has been used for the detection of volcanic SO<sub>2</sub> along with other satellite instruments including the Global Ozone Monitoring Experiment (GOME, 1995-2003; GOME-2, 2006-present), the Scanning Imaging Absorption Spectrometer for Atmospheric Chartography (SCIAMACHY; 2002-present), and the Solar Backscatter Ultraviolet instrument (SBUV; 1978-present) (Thomas and Watson, 2010). OMI's optimal combination of spatial, spectral, and temporal resolution has provided the capability of measuring SO<sub>2</sub> emissions from both erupting and passively degassing volcanoes from space.

Space-borne UV sensors measure the attenuation of UV radiation due to absorption by molecules of SO<sub>2</sub>, which can be used to retrieve total column amounts of this gas. The total column amount of a trace gas is defined as the amount of gas in a vertical column of unit cross-section extending from the Earth's surface to the top of the atmosphere, and is usually expressed as the equivalent thickness of pure gas at standard temperature and pressure (STP). Total column amounts of SO<sub>2</sub> are typically given in Dobson Units (DU; 1 DU =  $2.69 \times 10^{16}$  molecules cm<sup>-2</sup>) or in molecules cm<sup>-2</sup>, which can be easily converted to mass per unit area and hence SO<sub>2</sub> mass loading. Hereafter, total column amount will be referred to as vertical column density (VCD). Quantifying

column amounts of SO<sub>2</sub> from space is complicated due to various factors such as the variable UV radiation path length and changes in vertical distribution of the SO<sub>2</sub> in the atmosphere, the viewing geometry, absorption and scattering of UV radiation by other particles in the atmosphere and the surface, and cloud coverage. Although OMI has played a critical role in quantifying volcanic SO<sub>2</sub> gas emissions from space, validation studies need to be made on the data retrieval techniques, by comparisons with ground-based measurements, in order to make further improvements on the operational products that are being implemented into volcano monitoring programs.

Currently, two different algorithms are used for the operational retrieval of SO<sub>2</sub> from OMI measurements. The Band Residual Difference (BRD) algorithm, outlined in detail by (Krotkov et al., 2006), uses residuals from the operational OMI ozone algorithm (OMTO3) to estimate the SO<sub>2</sub> VCD. Residuals are the differences between measured and computed N-values ( $N = -100 \log_{10} (I/F)$ , where  $I$  = Earth radiance and  $F$  = solar irradiance; i.e., it is a scaled reflectance value), where the latter account for the effects of multiple scattering, ozone absorption, ring effect and surface reflectivity, but not SO<sub>2</sub> absorption. The BRD algorithm uses residuals from short wavelength pairs to estimate the SO<sub>2</sub> VCD because, in the presence of SO<sub>2</sub>, these are correlated with their respective differential SO<sub>2</sub> cross sections (Bhartia and Wellemeyer, 2002). The four UV wavelengths used to calculate the pair residuals are 310.80 nm, 311.85 nm, 313.20 nm, and 314.40 nm, which are sensitive to the detection of small SO<sub>2</sub> column amounts (due to strong SO<sub>2</sub> absorption at these wavelengths) and therefore appropriate for passively degassing volcanoes, although unsuitable for large SO<sub>2</sub> VCDs (due to saturation). The BRD algorithm was used by Carn et al. (2008), who presented daily measurements of

SO<sub>2</sub> from passively degassing volcanoes in Ecuador and Colombia. They showed how this algorithm permits automatic calculations of daily SO<sub>2</sub> burdens, and they were able to identify trends in degassing, which they attributed to opening and sealing processes in the volcanic conduits. However, the algorithm had various error sources that impacted the SO<sub>2</sub> retrieval accuracy. The development of more advanced SO<sub>2</sub> retrieval techniques, along with comparisons among each technique has led to improvements in satellite-based estimation of volcanic SO<sub>2</sub>.

The Linear Fit (LF) algorithm outlined in Yang et al. (2007) is an extended and more widely applicable version of the BRD algorithm. It uses 10 OMI wavelength bands, including those centered at the Earth-Probe TOMS wavelengths (McPeters et al., 1998), the four used for the BRD algorithm, and two additional bands in a spectral region unaffected by SO<sub>2</sub> absorption (Yang et al., 2007). The LF algorithm selects the UV wavelength bands whose residuals (as defined above) exhibit a linear response to changes in SO<sub>2</sub> VCD, thus avoiding the saturation issues that affect the BRD algorithm. These bands are used to compare measured and calculated top-of-the-atmosphere (TOA) radiances and simultaneously retrieve ozone, SO<sub>2</sub>, and effective surface reflectivity. Yang et al. (2007) made OMI SO<sub>2</sub> maps using the BRD and LF algorithms over the area of Sierra Negra volcano in the Galapagos Islands in order to explore their performance and limitations. They determined that the BRD and LF algorithms are in good agreement for SO<sub>2</sub> amounts less than ~10 DU, but the BRD algorithm underestimates VCDs for higher SO<sub>2</sub> loadings. The LF method is more valid than the BRD for high SO<sub>2</sub> loadings because it uses longer wavelengths that have a linear relationship with VCD up to ~100 DU. The BRD algorithm remains useful for passively degassing volcanoes since they

have lower SO<sub>2</sub> loadings. Although both algorithms need improvements for better accuracy (more specifically for monitoring eruptions), they have successfully measured global volcanic SO<sub>2</sub> loadings and are fast enough to generate SO<sub>2</sub> products in near real-time (Carn et al., 2009).

OMI SO<sub>2</sub> measurements require validation to ensure high-quality data. Validation can be achieved through comparisons with ground-based measurements, although this poses several problems including the differences in spatial averaging between satellite and ground-based measurements, cloud heterogeneity, and meteorological cloud interference. The first robust comparison of OMI volcanic SO<sub>2</sub> retrievals with ground-based measurements was achieved after the eruption of Okmok volcano (Aleutian Islands) on 18-20 July 2008 (Spinei et al., 2010). Spinei et al. (2010) used the Iterative Spectral Fit Algorithm (ISF), outlined by Yang et al. (2009), and the LF algorithm to obtain OMI SO<sub>2</sub> columns and compared them to coincident measurements taken by a ground-based multifunction differential optical absorption spectroscopy (MFDOAS) instrument over Pullman, WA. Their results showed good agreement between the 5 km VCD measurements under perfect meteorological conditions (clear skies), successfully validating OMI SO<sub>2</sub> retrieval data.

Carn et al. (2011) attempted validation of OMI volcanic SO<sub>2</sub> data from Ecuadorian and Colombian volcanoes with in-situ data collected by a NASA aircraft during the NASA Tropical Composition, Cloud and Climate Coupling (TC<sup>4</sup>) experiment. Even though they could not provide a robust validation, they found consistency between in-situ SO<sub>2</sub> concentrations and profiles and average SO<sub>2</sub> column amounts measured by

OMI. They suggested that better validation could be achieved by obtaining in situ measurements closer to the source volcano.

This investigation has three main objectives: a) we present comparisons between two methods used to calculate SO<sub>2</sub> loadings in volcanic plumes from OMI SO<sub>2</sub> data, in order to evaluate the relative accuracy of automatic vs non-automatic OMI analysis procedures that will permit improvements in data processing techniques for operational use (e.g., quantification of SO<sub>2</sub> emissions in near real-time); b) we attempt validation of OMI SO<sub>2</sub> data with ground-based SO<sub>2</sub> data obtained close to a currently strong source of volcanic SO<sub>2</sub> (Turrialba, Costa Rica) in order to assess the utility of the satellite measurements for monitoring passively degassing volcanoes; and c) in the light of these results we evaluate total SO<sub>2</sub> emissions from Turrialba since the beginning of its new eruptive phase and ongoing degassing activity, and speculate on how best to combine space-based and ground-based volcanic SO<sub>2</sub> measurements.

## **1.1 Geological Setting of the Study Area**

Turrialba is one of the largest and most active stratovolcanoes in the Central Cordillera of Costa Rica with an elevation of 3340 m a.s.l. (Figures 1 and 2). Located just 35 km northeast of the capital city of San Jose and even closer to other densely populated areas, this volcano poses a threat to the country's economic interests and aviation due to its recorded eruptive history, the surrounding steep slopes and valleys, and the regional meteorological conditions. It has been constantly degassing SO<sub>2</sub> since November 2001 and progressively increasing (Vaselli et al., 2010), with a dramatic

increase in March 2007 (Soto, 2010) that has been attributed to a shallow magmatic intrusion (Reagan et al., 2006), and renewed its eruptive activity during a series of short-lived phreatic explosions on January 5, 2010, which resulted in ashfall in San Jose (Martini et al., 2010). Validated SO<sub>2</sub> burdens and emission rates from this volcano are scarce and needed in order to monitor the changes in volcanic activity that may serve as eruption precursors and to further understand the magnitude and the extent of the effects on the climate and environment. Furthermore, SO<sub>2</sub> emission data can be used in conjunction with petrological data to infer volumes of degassed magma at depth, with implications for the volcanic plumbing system and the expected duration of activity. Turrialba volcano is an excellent target for validation of satellite data using ground based measurements due to its high elevation, relative ease of access, and persistent elevated SO<sub>2</sub> degassing.

### *1.1.1 Tectonic Setting*

Turrialba volcano is located at the southeastern terminus of the Central American Volcanic Arc. The tectonic framework of Costa Rica is complex due to the interaction of four plates and microplates: the Cocos, Caribbean, and Nazca plates, and the Panama block. The Costa Rican volcanic front is associated with the northeastward subduction of the Cocos plate beneath the Caribbean plate. The subduction angle changes drastically from 60° in the northwestern region to 30° in the southeastern region, where Turrialba is located (Alvarado et al., 2006).



**Figure 1:** Location of Turrialba volcano in Costa Rica, marked by the red star. Data Sources: Digital Elevation Models from CGIAR-CSI (Jarvis et al., 2008), and Boundary layer © 2011 Esri, DeLorme, NAVTEQ, TomTom, Automotive Navigation Data.

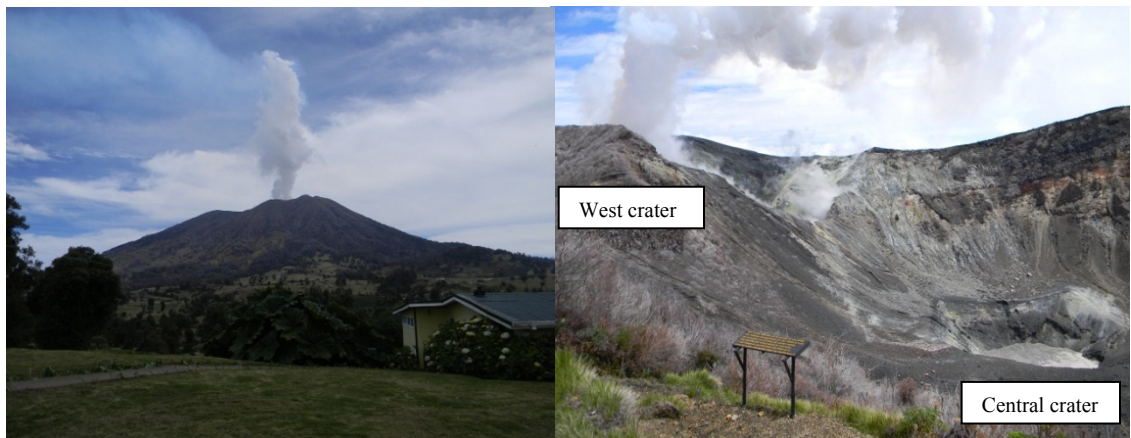


**Figure 2:** View of Turrialba volcano and its plume (Left); and view of the West and Central craters at the summit (Right).

### *1.1.2 Morphostructural Features*

The Turrialba volcanic edifice overlies Tertiary eroded volcanoes (Bellon and Tournon, 1978). This volcanic edifice consists of an elliptical caldera (~2 km diameter) facing northeast, which contains three well-defined interior craters labeled as west, central, and east. The west crater is associated with the most recent magmatic eruptive activity (Reagan et al., 2006). Volcanic activity in the central crater consists primarily of fumarolic gas emissions, and it contains an intermittent water body due to high precipitation volumes in the region. The east crater is not associated with recent eruptive activity. The volcanic edifice also contains three exterior peaks with the names Cerro San Carlos (north), Cerro San Enrique (east), and Cerro San Juan (southwest) which consist mainly of silicic andesite lavas and andesitic to basaltic-andesite pyroclastic deposits, and two cinder cones named Tiendilla and El Armado of basaltic-andesite composition (Reagan et al., 2006).

### *1.1.3 Stratigraphic Record and Eruptive History*

Several eruptions have been preserved in the stratigraphic record of Turrialba volcano. Soto (1988) presents a morpho-structural map of Turrialba volcano in which he defines 17 geologic units. Reagan et al. (2006) described the geology and stratigraphic record of Turrialba's summit region and defined 15 stratigraphic units, dividing them into pre- and post- glaciation periods (Table 1). The pre-glaciation period (Late Pleistocene to Holocene) volcanic activity at Turrialba was characterized by effusive andesitic to dacitic lava eruptions, while the volcanic activity since the post-glaciation period (after 9300



B.P.) was predominantly explosive and generally ranging from basaltic-andesitic to andesitic composition (Reagan et al., 2006). The most recent eruptive activity (January, 2010 to August, 2011) has consisted of phreatic eruptions with tephra fall and continuous gas emissions (Table 2).

**Table 1:** Stratigraphic record at Turrialba volcano (after Reagan et al., 2006). <sup>(1)</sup>Based on Radiocarbon Dating; <sup>(2)</sup>Based on K-Ar dating

Unit	Age	Lithology
Unit 1	1864-1866 A.D.	Basaltic lava flows, lahars, tephra/ash fall (with lapilli), pyroclastic surges
Unit 2	?	Basaltic-andesite pyroclastic deposits
Unit 3	~1500 B.P. <sup>(1)</sup>	Basaltic-andesite, andesitic and dacitic pyroclastic surges, tephra fall
Unit 4	2330-1860 B.P. <sup>(1)</sup>	Andesitic tephra fall, pyroclastic flows, pyroclastic surges
Unit 5	2800 B.P. <sup>(1)</sup>	Andesitic ash and lapilli (pyroclastic surge?)
Unit 6	~3300 B.P. <sup>(1)</sup>	Basalt and Basaltic-andesite ashfall (with lapilli), pyroclastic fall
Unit 7	~3370 B.P. <sup>(1)</sup>	Basaltic-andesite pyroclastic falls, pyroclastic surges, and ash fall
Unit 8	9300 <sup>(1)</sup> B.P.	Andesitic and dacitic lava flows, dacitic pyroclastic flows
Unit 9	9300-50,000 <sup>(2)</sup> B.P.	Andesitic lava flows
Unit 10	Late Pleistocene to Holocene(Pre-erosional glaciation)	Basaltic-andesite lava flows
Unit 11	Late Pleistocene to Holocene(Pre-erosional glaciation)	Andesitic pyroclastic breccias
Unit 12	Late Pleistocene to Holocene(Pre-erosional glaciation)	Dacitic lava flows and breccias
Unit 13	Late Pleistocene to Holocene(Pre-erosional glaciation)	Basaltic-andesite lava flows and breccias
Unit 14	Late Pleistocene to Holocene(Pre-erosional glaciation)	Basaltic, andesitic and dacitic lava flows
Unit 15	Late Pleistocene to Holocene(Pre-erosional glaciation)	Basaltic, andesitic and dacitic lava flows

**Table 2:** Eruptive history of Turrialba volcano. Compiled data from the Global Volcanism Program ©(Simkin and Siebert, 2002-2011a). <sup>1</sup>Based on Radio Carbon Dating; <sup>2</sup>Based on Tephrochronology; <sup>3</sup> Uncertain Eruption; <sup>4</sup> Based on Historical Records. VEI stands for Volcanic Explosivity Index.

Date	VEI	Description of Activity
7260 BC ± 300 <sup>(1)</sup>		Central vent eruption, explosive eruption; Lava volume: $4.5 \times 10^9 \text{ m}^3$ ; Area of activity: East summit crater; Pyroclastic flow(s), lava flow(s)
1420 BC ± 300 <sup>(1)</sup>		Central vent eruption, explosive eruption, phreatic explosion(s)
1120 BC ± 200 <sup>(2)</sup>		Central vent eruption, explosive eruption, phreatic explosion(s)
830 BC ± 150 <sup>(1)</sup>		Central vent eruption, explosive eruption; Pyroclastic flow(s)
40 AD ± 50 <sup>(1)</sup>	4	Plinian; Tephra volume: $4 \times 10^8 \text{ m}^3$ ; Pyroclastic flow(s), lava flow(s)?, lava dome extrusion?
640 AD ± 40 <sup>(1)</sup>		Central vent eruption, phreatic explosion(s); Pyroclastic flow (s),
1350 <sup>(1)</sup>		Central vent eruption, explosive eruption
1723 <sup>(3)</sup>	1	Central vent eruption
1847 <sup>(3)</sup>		Central vent eruption
1853 <sup>(4)</sup>	2	Vulcanian to Strombolian; Central vent eruption
May 1855 <sup>(4)</sup>	2	Vulcanian to Strombolian; Central vent eruption
1861 <sup>(3)</sup>		Eruption uncertain (central vent eruption)
August 17, 1864 <sup>(4)</sup>	2	Vulcanian to Strombolian eruption, Phreatic explosion(s); Area of activity: Central and western summit craters; Pyroclastic flow(s)
1866 <sup>(4)</sup>	3	Vulcanian to Strombolian eruption, Phreatic explosion(s); Tephra Volume: $10^7 \text{ m}^3$ ; Area of activity: Central and western summit craters; Pyroclastic flow(s), lahar(s)
Jan 5, 2010 <sup>(4)</sup>	2	Western crater explosive eruption, phreatic explosion(s), tephra fall; Area of activity: Southwestern crater
July 24, 2010 <sup>(3)</sup>		Western crater eruption, tephra fall
August 15, 2010 <sup>(4)</sup>		Western crater eruption, tephra fall
January 14, 2011 <sup>(4)</sup>		Western crater eruption, tephra fall

## 1.2 Previous Work on Turrialba

Physical and chemical changes have been studied at Turrialba volcano since 1998 and have been divided into three different stages of volcanic activity (Vaselli et al., 2010). The first stage took place from 1998 to 2001 and consisted of hydrothermal activity, characterized by low fumarolic emissions ( $\text{H}_2\text{O}$ ,  $\text{CO}_2$ ,  $\text{H}_2\text{S}$ ,  $\text{HCl}$ ,  $\text{HF}$ ) from the summit craters (Central and West) due to dissolution of magmatic fluids in the main hydrothermal reservoir with the exception of low solubility compounds. The second stage occurred from 2001 to 2007 and consisted of hydrothermal-magmatic activity, characterized by increased fumarolic gas fluxes (including the appearance of  $\text{SO}_2$ ), seismic activity, and ground deformation. The present third stage began in 2007 and consists of magmatic-dominated activity, characterized by a remarkable increase in gas fluxes (increased  $\text{SO}_2$ ) from the summit craters (Central and West) and areas distant to it, the opening of new vents around the volcano, and an increase in heat flux. These stages could reflect either a cycle regulating the balance between hydrothermal and magmatic systems, or the rejuvenation of magmatic/volcanic activity (Vaselli et al., 2010).

Martini et al. (2010) collated the available geophysical, geochemical, and geodetic data for Turrialba volcano during the period between 1990 and 2008. They confirmed the three phases of activity that were previously identified by Vaselli et al., (2010), but they also suggested the possibility of a magmatic intrusion being the cause of several seismic swarms that occurred in the area during 2007. Improvements in monitoring efforts for this volcano are needed in order to understand the magmatic processes occurring and the possible hazards associated with the volcanic activity.

Sampling indicator gases may provide signals of impending eruptions. Remote sensing tools are used to measure gas emissions in order to prevent exposure to the hazards posed by sampling them in proximity to the vent. The Utilization of Lightweight In situ Sensors and remote Sensing to study active volcanic Emissions Sites (ULISSES) system is a mass spectrometer-based gas analyzer that has been deployed from both ground and airborne platforms at Turrialba volcano. In the investigation presented by Diaz et al. (2010), masses and ratios were obtained from ULISSES for several days between 2009 and 2010, including before and after the January 2010 series of phreatic eruptions at Turrialba. The data obtained by ULISSES during their January 19, 2010 field deployment were compared to SO<sub>2</sub> masses obtained by OMI during the same day. According to the data shown in their investigation, OMI measured high SO<sub>2</sub> masses during the same time that ULISSES measured two SO<sub>2</sub> peaks. However, the information provided in their investigation was incomplete and used incorrectly for validation of the instruments because OMI detected higher SO<sub>2</sub> amounts in comparison with the lower SO<sub>2</sub> amounts measured by the ULISSES system.

## **2. The Ozone Monitoring Instrument: Comparison of SO<sub>2</sub> mass calculations**

### **2.1 The Ozone Monitoring Instrument**

NASA's Earth Observing System (EOS) Aura satellite was launched on July 15, 2004 into a polar sun-synchronous orbit, providing latitudinal coverage from 82°N to 82°S each day. It orbits at 705 km altitude with a 16-day repeat cycle and with a local equator crossing time (ascending node) of approximately 1:45 P.M (OMI-Team, 2011). OMI is one of four instruments onboard the Aura satellite and it is used for the purposes of this investigation. OMI is a wide-angle, non-scanning, nadir-viewing hyperspectral imaging spectrograph that has two channels for measurements of backscattered radiance: a) the UV channel; and b) the VIS channel. The UV channel is divided into two bands, UV-1 and UV-2, which measure wavelengths from 264-311 nm and 307-383 nm respectively. The VIS channel measures from 349-504 nm. OMI measures the backscattered radiance with an instantaneous field of view (IFOV) of 115° in the cross-track direction (~2600 km on the ground) and 1° in the flight (along-track) direction, producing a nadir ground pixel size of 13 x 24 km<sup>2</sup>. It uses a two-dimensional Charge-Coupled Device (CCD) that obtains both spatial and spectral data simultaneously, with an image integration time of 0.4 seconds. OMI is designed to provide accurate measurements of total column ozone, ozone profile, surface UV-B flux, aerosol and cloud characteristics, and the column amounts of gases such as SO<sub>2</sub>, NO<sub>2</sub>, BrO, HCHO, and OCIO (Levelt et al., 2006).

## 2.2 OMI Data Analysis

OMIplot software was used throughout this investigation to visualize and analyze OMI Level-2 SO<sub>2</sub> data products (free data products available online through <http://mirador.gsfc.nasa.gov/cgi-bin/mirador/collectionlist.pl?keyword=omso2>). The software runs with the Interactive Data Language (IDL) and uses various algorithms for data processing (Carn, 2011). The operational LF algorithm was used to generate daily maps of SO<sub>2</sub> VCDs for the time range from January 1, 2010 to December 31, 2010 for the Nicaragua and Costa Rica region. Operational LF OMI SO<sub>2</sub> retrievals are currently provided for four different a-priori SO<sub>2</sub> vertical profiles represented by center of mass altitudes (CMA): planetary boundary layer (PBL; CMA = 0.9 km), lower troposphere (TRL; CMA = 2.5 km); mid-troposphere (TRM; CMA = 7.5 km) and upper troposphere/lower stratosphere (STL; CMA = 17.5 km). In the absence of accurate daily SO<sub>2</sub> plume altitude information, we use the CMA closest to the altitude of the volcanic vent (TRL for Turrialba). Volcanic SO<sub>2</sub> cloud masses were calculated in units of kilotons (kt; 1 kt = 10<sup>3</sup> metric tons) using two methods: a) the automatic Band Residual Index technique (BRI); and b) the manual Normalized Cloud-mass technique (NCM). The BRI technique is currently used operationally to calculate SO<sub>2</sub> burdens in volcanic emissions detected by OMI, with the results reported on images posted on the NASA Global SO<sub>2</sub> Monitoring website (<http://so2.gsfc.nasa.gov>). Here, we compare results from the BRI and NCM techniques to investigate the accuracy of the SO<sub>2</sub> burdens derived from the automatic BRI technique.

### 2.2.1 Band Residual Index

The first step in the automated SO<sub>2</sub> mass calculation procedure is to separate OMI pixels containing real SO<sub>2</sub> (i.e., ‘plume’ pixels) from background noise. The BRI technique utilizes the OMTO3 residuals at the BRD algorithm wavelengths (section 1; Figure 3) to identify plume pixels (Figure 4). Due to the placement of the BRD wavelengths at maxima and minima in the SO<sub>2</sub> absorption cross-section, OMTO3 residuals exhibit a characteristic relationship in the presence of SO<sub>2</sub>, i.e., residuals will be largest where SO<sub>2</sub> absorption is strongest, and lowest where it is weakest. Hence, for the four BRD wavelengths (Figure 3) we use the following relationship to identify plume pixels (R denotes residual):

$$R_{310.8} - R_{311.85} > 0.1 \quad (\text{pair 1})$$

$$R_{311.85} - R_{313.2} < 0 \quad (\text{pair 2})$$

$$R_{313.2} - R_{314.4} > 0.1 \quad (\text{pair 3})$$

The 0.1 threshold for the pair 1 and pair 3 residuals is an empirical one derived from offline examination of residuals for many OMI pixels containing SO<sub>2</sub>. Following identification of plume pixels, the total SO<sub>2</sub> burden in the scene (M, in kt) is calculated by summing the SO<sub>2</sub> mass in each plume pixel:

$$M = 0.0000285 \sum_{i=1}^n VCD_i A_i \quad (1)$$

where  $A$  is the pixel area in  $\text{km}^2$ ,  $\text{VCD}$  is in DU, and 0.0000285 is the conversion factor from DU to kt units. Daily OMI  $\text{SO}_2$  maps were generated with coordinates from  $7^\circ\text{N}$  to  $13^\circ\text{N}$  and  $88^\circ\text{W}$  to  $82^\circ\text{W}$ , and automatically analyzed using the BRI technique. Volcanic  $\text{SO}_2$  burdens were thus obtained using the TRL  $\text{SO}_2$  columns for the entire area under analysis during the previously mentioned time range.

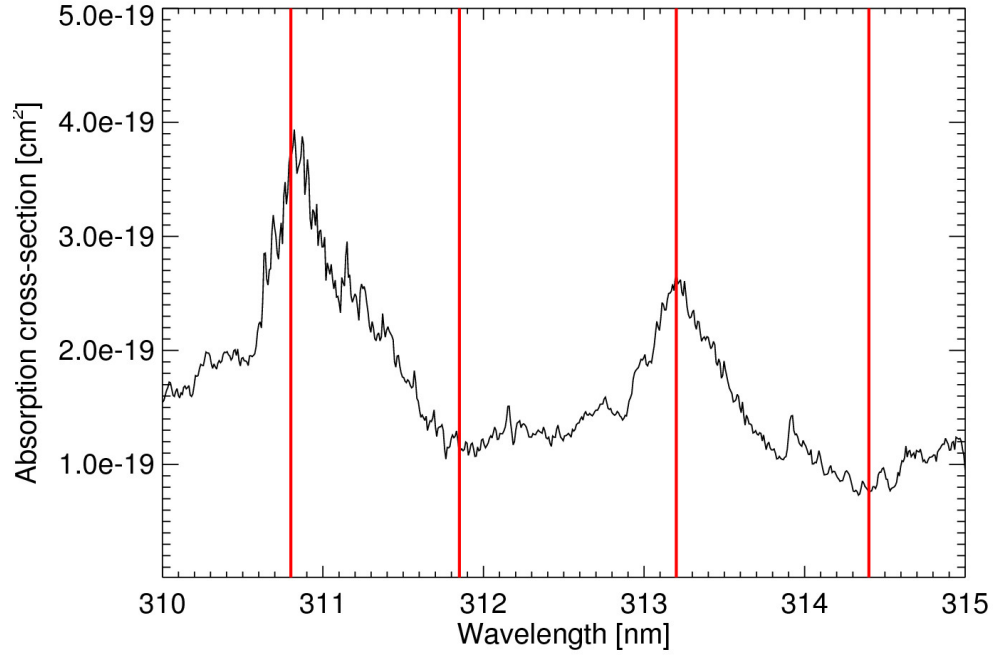


**Figure 3:** High resolution  $\text{SO}_2$  absorption cross-section (Vandaele et al., 1994) from 310-315 nm with BRD wavelengths indicated (red lines).



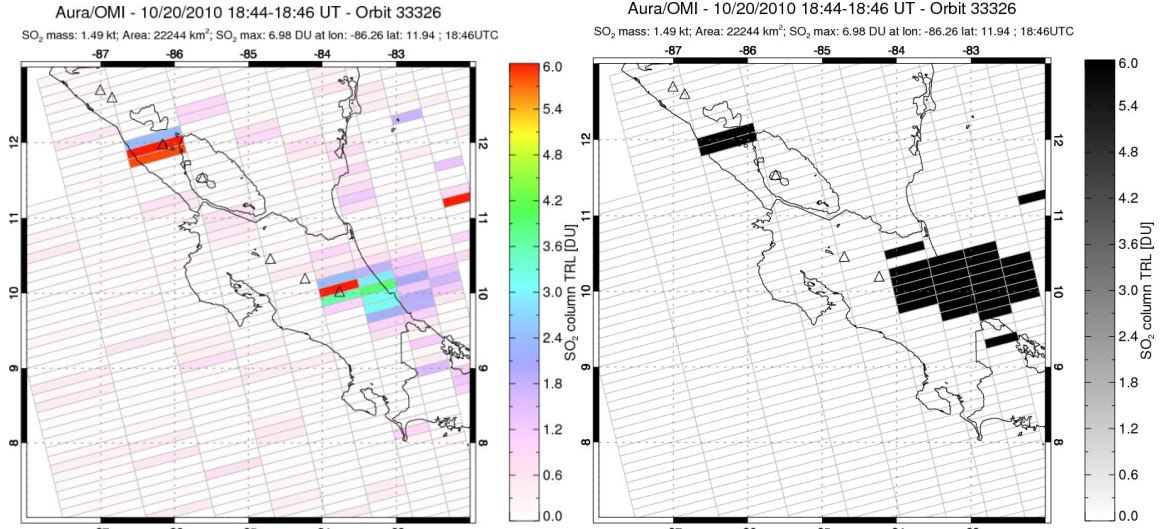


**Figure 4:** Example of volcanic SO<sub>2</sub> pixel selection for an OMI daily image using the BRI technique.

### 2.2.2 Normalized Cloud-mass

Daily OMI SO<sub>2</sub> maps were generated with coordinates from 8°N to 12°N and 88°W to 80°W, and manually analyzed. The region under analysis for this technique is smaller than that of the BRI to reduce the addition of volcanic SO<sub>2</sub> sources from other nearby volcanoes. Assuming a volcanic plume at an altitude of ~3 km (i.e., TRL SO<sub>2</sub> columns), uncorrected SO<sub>2</sub> masses were retrieved by selecting a box containing Turrialba's volcanic plume (Figure 5). In order to correct for OMI SO<sub>2</sub> background noise, the National Oceanic and Atmospheric Administration (NOAA) Real-time Environmental Applications and Display System (READY) web-based system (Rolph, 2003) was used to retrieve wind data from the study area in order to identify regions with volcanic SO<sub>2</sub>-free background conditions (i.e., upwind of the volcano) (See Appendix A). Two SO<sub>2</sub>-free background regions adjacent to the volcanic region with similar

meteorological conditions (similar OMI cloud fractions) and coverage area were selected and averaged to obtain a background SO<sub>2</sub> mass (Figure 5). The corrected SO<sub>2</sub> mass (SO<sub>2</sub><sup>CM</sup>) was then calculated using the following equation:

$$SO_2^{CM} = SO_2^{UM} - ((Area^{BG\ SO_2} / Area^{U\ SO_2}) \times SO_2^{BGM}) \quad (2)$$

where SO<sub>2</sub><sup>UM</sup> is the uncorrected SO<sub>2</sub> mass in Turrialba's volcanic plume, Area<sup>BG SO<sub>2</sub></sup> is the average area of the two background regions, Area<sup>U SO<sub>2</sub></sup> is the area of the region containing the volcanic plume, and SO<sub>2</sub><sup>BGM</sup> is the average of the two background SO<sub>2</sub> masses.

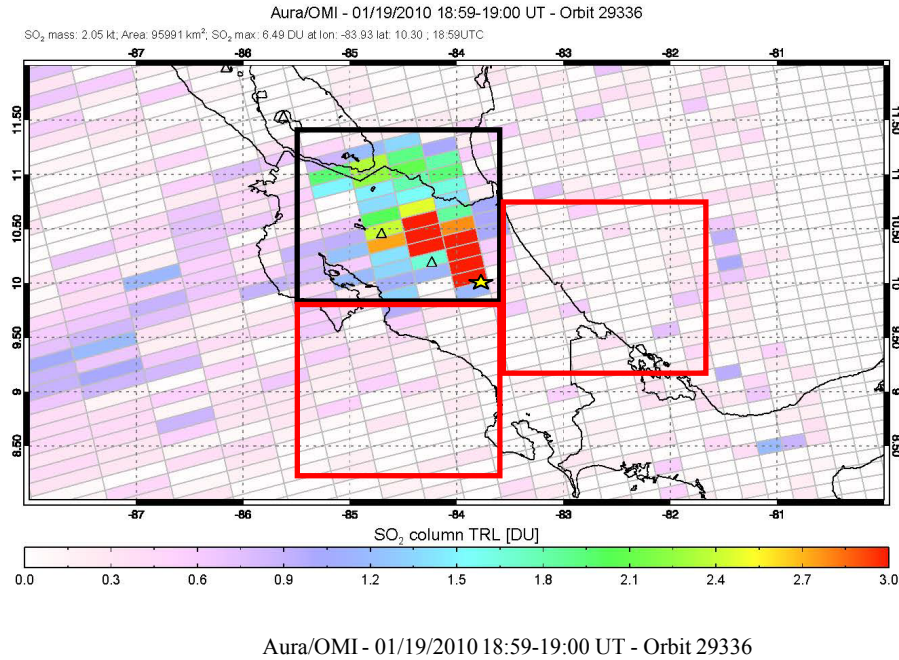


**Figure 5:** Example of a daily OMI image of Costa Rica with the satellite almost at nadir. The yellow star indicates the location of Turrialba volcano and the triangles are nearby volcanoes. The black box contains Turrialba's volcanic plume, and the two red boxes contain background noise.

### *2.2.3 SO<sub>2</sub> Emission Rates from Cumulative Plots*

Cumulative SO<sub>2</sub> plots have been used to estimate SO<sub>2</sub> burdens from different sources for a given time range (Carn et al., 2008). Using the SO<sub>2</sub> masses obtained with the NCM and BRI techniques, we calculated the cumulative SO<sub>2</sub> burden from Turrialba volcano during the year 2010. The slope of the cumulative mass curve provides an estimate of the average daily SO<sub>2</sub> emission from the volcano but it is not the true volcanic SO<sub>2</sub> emission rate since the measured SO<sub>2</sub> masses do not account for SO<sub>2</sub> depletion in the atmosphere. Emission rates from the cumulative plots can be calculated if an SO<sub>2</sub> lifetime is known.

Monthly average OMI TRL SO<sub>2</sub> maps were generated for the area during the same time period (Appendix B) to estimate the monthly average lifetime of SO<sub>2</sub>. Daily wind speed (m/s) data were obtained from NOAA's READY archived meteorology database and used to calculate a monthly average wind speed value for the volcanic plume. Assuming a constant wind speed, and a continuous and linear wind direction, the distance (km) traveled per day (D<sub>TPD</sub>) by the volcanic plume with a constant wind speed (v) was calculated using:

$$D_{TPD} = (86400 \times v)/1000 \quad (3)$$

where 86400 is the number of seconds in one day and 1/1000 is the conversion factor from meters to kilometers. Using this equation and the measurement from the distal end of the visible volcanic SO<sub>2</sub> plume with respect to the volcanic source (D<sub>FP</sub>) (See Figure

6), the lifetime ( $\tau$ ) of volcanic  $\text{SO}_2$  from Turrialba was calculated for each image under analysis:

$$\tau = D_{\text{FP}}/D_{\text{TPD}} \quad (4)$$

These  $\text{SO}_2$  lifetimes are considered to be the maximum amounts since  $\text{SO}_2$  depletion is occurring before the distal end of the plume, as observed in the images by the diminishing  $\text{SO}_2$  concentration as the plume is further from the volcano (even though some  $\text{SO}_2$  molecules are surviving the trip). Using the previously obtained daily average  $\text{SO}_2$  mass ( $M$ ) from the volcano for 2010 (slope of the cumulative plot) from both the NCM and BRI techniques,  $\text{SO}_2$  emission rates were estimated thus:

$$\text{SO}_2 \phi = M/ \tau \quad (5)$$

Since the  $\text{SO}_2$  lifetime is the maximum amount, the resulting  $\text{SO}_2$  flux represents the minimum emission rate for the year 2010.

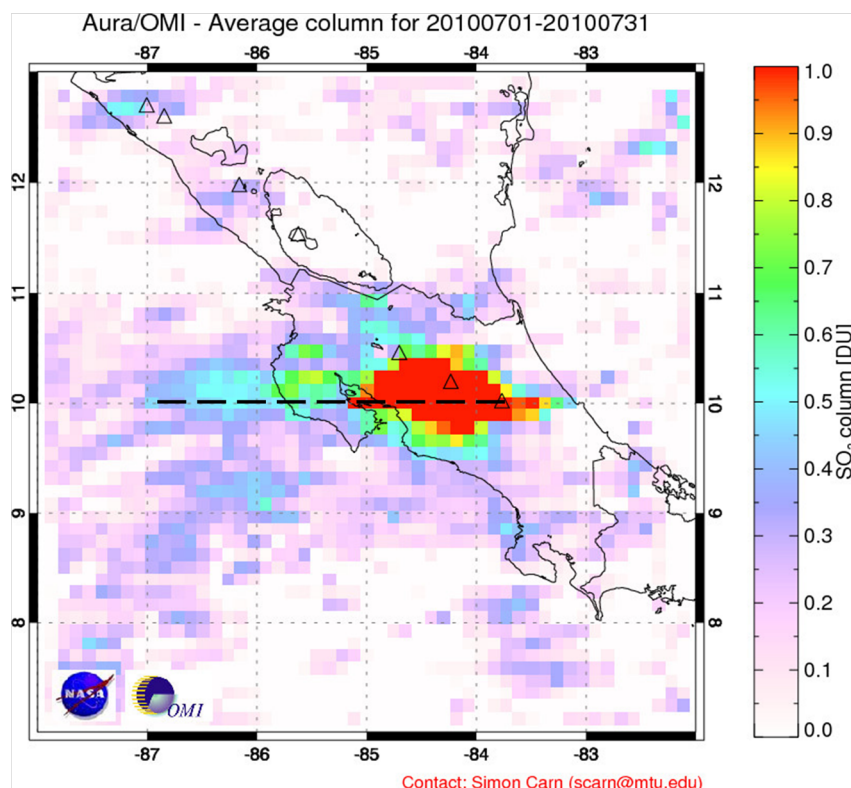


**Figure 6:** Example of OMI monthly SO<sub>2</sub> average plot for July, 2010. The black dashed line represents the volcanic plume trajectory and its distal end used for the SO<sub>2</sub> lifetime calculation.

## 2.3 Results and Discussion

### 2.3.1 Band Residual Index vs. Normalized Cloud-mass

The daily SO<sub>2</sub> burdens from Turrialba volcano obtained using both the NCM and BRI techniques were plotted against each other in a time-series chart for further analysis (Figure 7). The plot reveals similar patterns and demonstrates a generally good agreement between the techniques. The BRI, however, occasionally showed higher SO<sub>2</sub> masses for two main reasons: a) days were other nearby volcanoes (e.g., Poas, Arenal, Concepcion, Masaya, Telica, San Cristobal) were emitting SO<sub>2</sub>, being unable to

distinguish between the different volcanic SO<sub>2</sub> sources in the area under analysis; and b) inclusion of more pixels containing background SO<sub>2</sub> noise due to a larger analysis area. This could be ameliorated by reducing the size of the analyzed geographic region. With the NCM technique this error is reduced, since the user can adjust the analysis region according to the extent of Turrialba's plume. However, uncertainties still occur due to possible volcanic SO<sub>2</sub> emissions from Poas, which are often difficult to exclude from the analysis due to its proximity to Turrialba, and the spatial resolution of the generated images. On days that the instrument was not at nadir, the average SO<sub>2</sub> calculated per pixel covers a greater area, making it sometimes impossible to distinguish between the two volcanic sources and therefore obtaining an SO<sub>2</sub> average for both volcanoes.

In the period from May to November 2010, the BRI technique consistently underestimated the SO<sub>2</sub> burden relative to the NCM, which we attribute to the rainy season in Costa Rica. Underestimation of volcanic SO<sub>2</sub> from OMI LF retrievals have been shown to occur when the SO<sub>2</sub> plume is located either below or mixed with meteorological clouds (Yang et al., 2007). Since the area under analysis using the BRI technique is larger than the NCM, the former likely includes a higher amount of cloudy pixels in the analysis, which could result in underestimation of the SO<sub>2</sub> burden (more specifically during the wet season). It is also possible that the residuals used to identify plume pixels by the BRI technique are not as robust in the presence of meteorological cloud contamination.

A linear relationship between the NCM and BRI SO<sub>2</sub> burdens is illustrated in Figure 8, showing a general agreement of ~91% (as obtained from the slope calculation) although the correlation coefficient was 0.6 due to the rainy season which tends to fall

under the trendline. SO<sub>2</sub> masses for the 2010 dry season show a better general agreement with a correlation coefficient of 0.7 (Figure 9). These results demonstrate that, although improvements still need to be made in future algorithms to account for errors such as noise from different volcanic sources and meteorological conditions, the automatic BRI technique appears suitable for operational use when compared to the manual NCM technique, and can be used to calculate SO<sub>2</sub> burdens in near real-time with minimum input effort. This permits rapid generation of long-term volcanic SO<sub>2</sub> mass time-series that can be used for volcano monitoring worldwide.

### *2.3.2 OMI Cumulative Plot Technique*

The minimum cumulative SO<sub>2</sub> mass measured by OMI at Turrialba for the year 2010 resulted in 245 and 275 kt using the NCM and BRI respectively (See Figure 10). The average daily volcanic SO<sub>2</sub> burden for 2010 provided by the gradient of the cumulative plot yields similar results for both SO<sub>2</sub> mass calculation techniques, 718 t/d for the NCM and 712 t/d for the BRI, with a difference of 0.7%. These results were used along with the calculated average SO<sub>2</sub> lifetime for 2010, 0.95 days, to estimate the daily average SO<sub>2</sub> emission rates during the same year (Table 3). Emission rates using the NCM technique resulted in 757 t/d and the BRI in 751 t/d, with a difference of 0.8%. These results were used to quantify the SO<sub>2</sub> emitted by Turrialba volcano for the year 2010, with a total of 276 kt/y and 274 kt/y using the NCM and BRI respectively. This estimation represents the minimum amount of Turrialba's volcanic SO<sub>2</sub> input into the troposphere, demonstrating the utility of satellite measurements that could be used for volcano monitoring purposes and for climate modeling analysis.

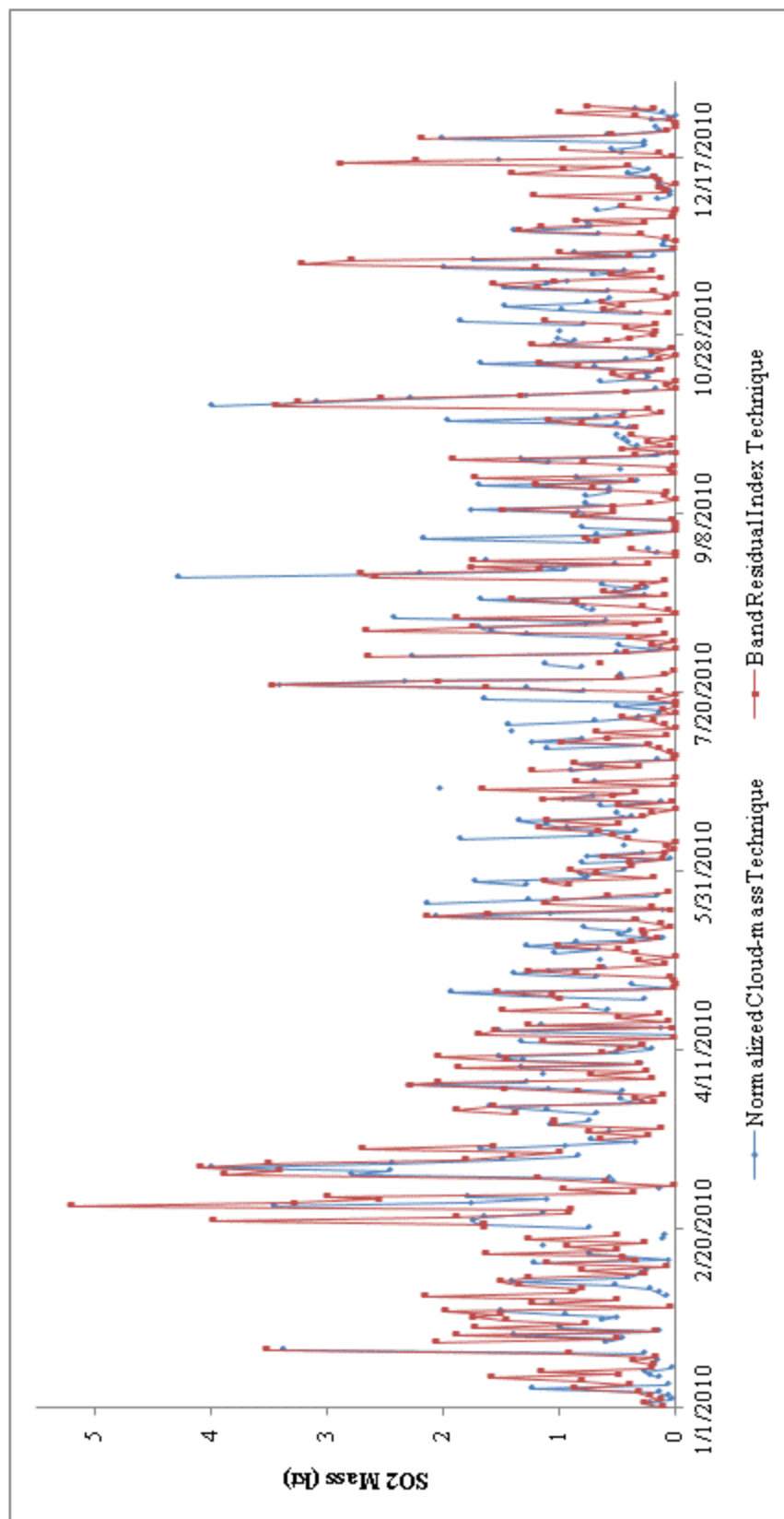


**Figure 7:** Turrialba NCM and BRI SO<sub>2</sub> mass time series plot for the year 2010.



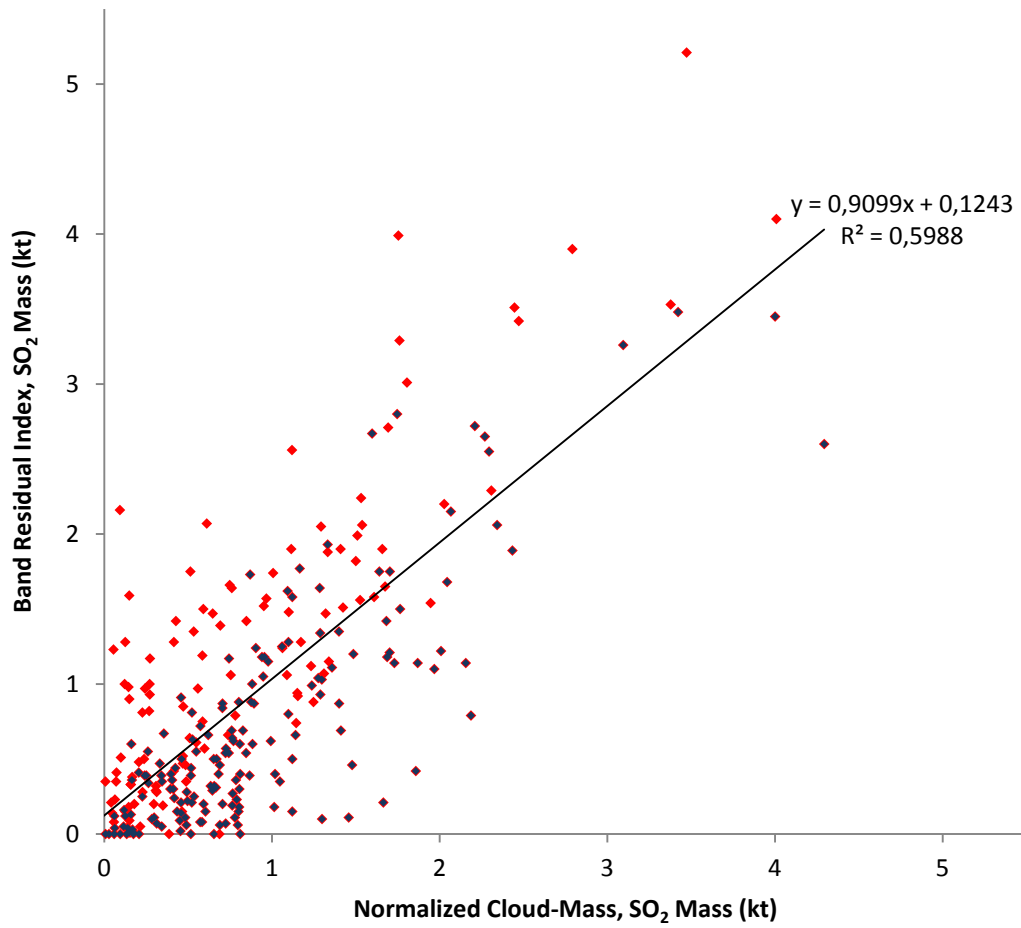


**Figure 8:** BRI SO<sub>2</sub> masses plotted against the NCM SO<sub>2</sub> masses for the year 2010 showing a linear relationship. Data for the rainy season (May-November) are shown as dark symbols, while the dry season data (December-April) are shown as red symbols.

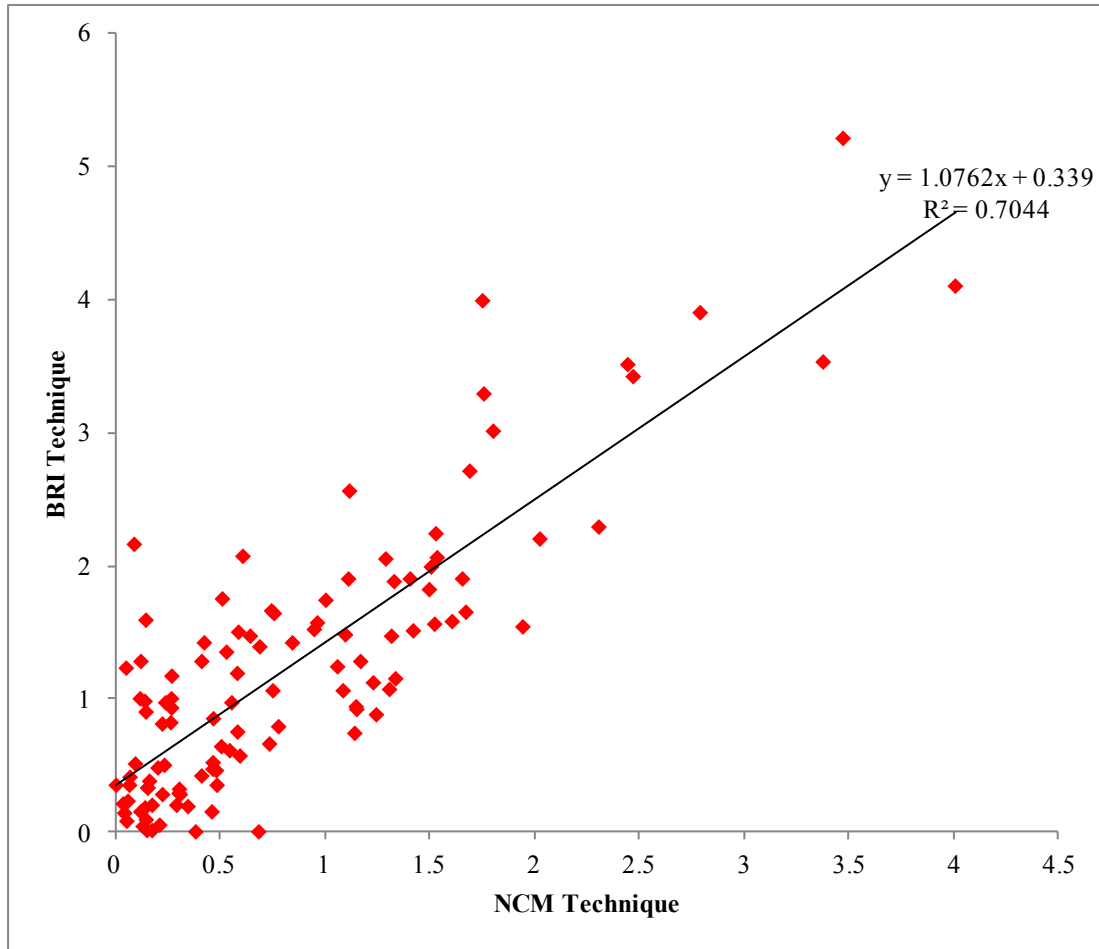


**Figure 9:** BRI SO<sub>2</sub> masses plotted against the NCM SO<sub>2</sub> masses for the 2010 dry season showing a linear relationship

SO<sub>2</sub> masses have been used in other studies for OMI validation (e.g., Pinardi et al., 2010), but our results show that the obtained SO<sub>2</sub> emission rates are higher than the obtained SO<sub>2</sub> masses. The results are considered to be minimum values since there are several data gaps due to OMI spatial zoom mode measurements (one day per month; SO<sub>2</sub> data are not currently produced on these days), data gaps due to the OMI ‘row anomaly’ that affects part of the CCD detector (<http://www.knmi.nl/omi/research/product/rowanomaly-background.php>), and days on

which cloud coverage did not permit the detection of Turrialba's volcanic plume. More days were analyzed using the BRI technique than with the NCM technique since the former used a larger analysis region, resulting in fewer data gaps. Since the BRI technique does not distinguish between different volcanic sources, the results potentially include SO<sub>2</sub> emissions from all actively degassing volcanoes in the Costa Rica and Nicaragua (although Turrialba is currently the strongest SO<sub>2</sub> source in the region under analysis), plus SO<sub>2</sub> clouds from other volcanoes that may drift across the region. The NCM technique is more specific to Turrialba volcano with less interference from SO<sub>2</sub> from other volcanoes.

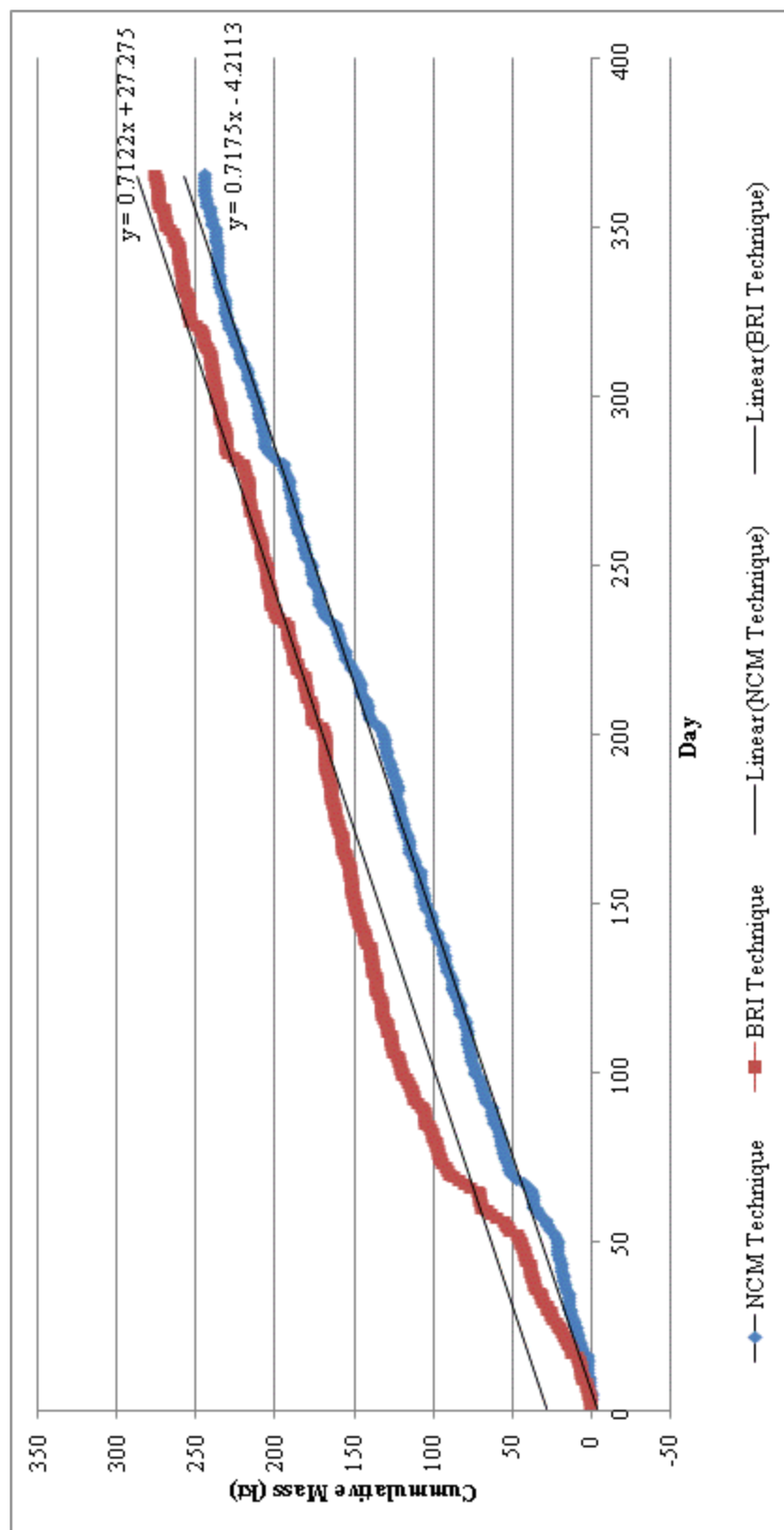


**Figure 10:** Cumulative SO<sub>2</sub> mass for Turrialba volcano during the year 2010.

**Table 3:** Maximum volcanic SO<sub>2</sub> lifetime per month and OMI cumulative SO<sub>2</sub> emissions for Turrialba during the year 2010

Month	SO <sub>2</sub> Lifetime (days)	Month	SO <sub>2</sub> Lifetime (days)	Month	SO <sub>2</sub> Lifetime (days)
January	0.767702	May	0.873515	September	1.525453
February	0.670198	June	0.649695	October	1.17969
March	1.024203	July	0.919026	November	0.604296
April	0.970534	August	1.70394	December	0.492273
<b>Average SO<sub>2</sub> Lifetime (days): 0.948377</b>					

	NCM	BRI
<b>OMI Daily Average SO<sub>2</sub> Mass (t)</b>	717.5	712.2
<b>OMI Daily Average SO<sub>2</sub> Flux (t/d)</b>	756.5555	750.967
<b>OMI Yearly SO<sub>2</sub> Flux (kt/yr)</b>	276	274

### **3. Comparisons between OMI SO<sub>2</sub> Data and Mini-DOAS measurements at Turrialba volcano**

#### **3.1 Mini-DOAS Data Collection**

A mini-DOAS instrument consists of a compact spectrograph fiber-coupled to a scanner unit that uses scattered sunlight in the UV region to derive path-integrated concentrations of various atmospheric gases (Galle et al., 2003), and in this case used for the quantification of volcanic SO<sub>2</sub> emissions (Figure 11). Two versions of these instruments were used at Turrialba volcano for the collection of ground-based SO<sub>2</sub> data: a) Michigan Technological University's (MTU) Resonance Mini-DOAS; and b) the Network for Observation of Volcanic and Atmospheric Change (NOVAC; Galle et al., 2010) mini-DOAS. For this investigation, the stationary measurement strategy was used to collect SO<sub>2</sub> data, which consisted of finding a fixed position on the ground (ideally directly beneath the volcanic plume) where the instrument scans a vertical plane perpendicular to the direction of plume transport (Figure 11). The data obtained by these instruments were used to estimate SO<sub>2</sub> emission rates and the results were then compared with several OMI analysis techniques used to derive SO<sub>2</sub> emission rates from satellite measurements of SO<sub>2</sub> VCD.

##### *3.1.1 MTU Resonance Mini-DOAS*

The system is based on an Ocean Optics USB4000 spectrograph that employs a linear CCD array that recovers a spectrum from 285 to 450 nm. This is connected to a scanner unit, which consists of a slot for insertion of SO<sub>2</sub> calibration cells, an elliptical

mirror that rotates between  $-60^\circ$  to  $60^\circ$  and is controlled electronically by the operating software, and a telescope with a 25 mm focal length lens to focus the incoming light into the fiber optic cable that is coupled to the spectrometer (Resonance, 2007). The instrument was set to measure a spectrum every  $3-5^\circ$  (steps) with integration periods of 1-1.2 seconds. These parameters are shown in Table 4, along with data collected from this instrument that we use for subsequent analysis.

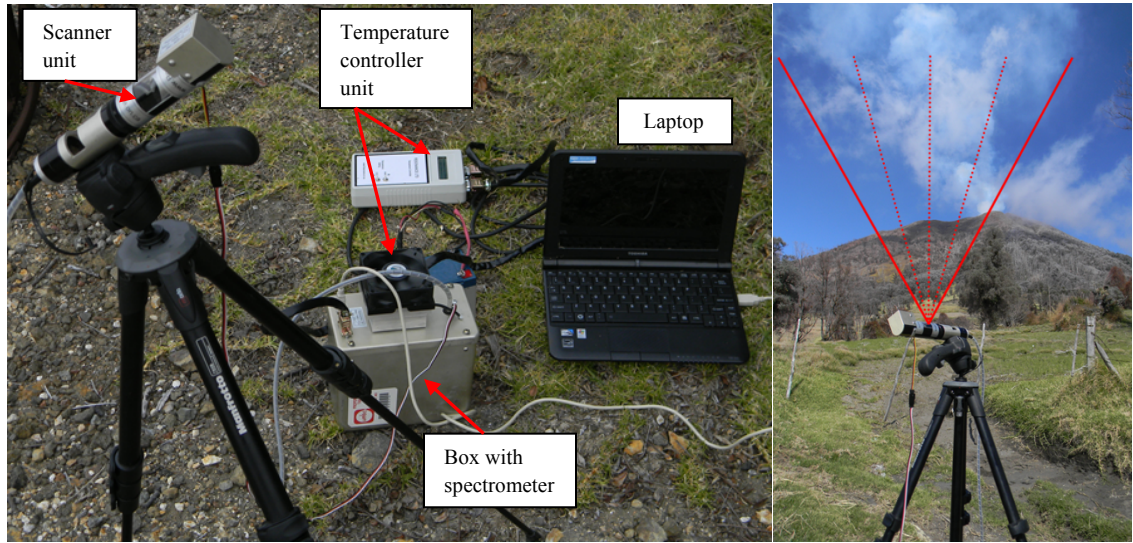


**Figure 11:** Mini-DOAS system components (Left); and an example of the stationary measurement strategy with red lines representing the scanning under Turrialba's plume (Right)

**Table 4:** Available data and parameters used during the mini-DOAS field deployment.

Date	Location Coordinates (USR)	Time Range (UTC)	Integration Period (s)	Minimum, Maximum Angles ( $^\circ$ )	Steps ( $^\circ$ )
7/23/2010	0559907,0222708	14:43-14:47	1	-40,40	3.3
7/23/2010	0559907,0222708	14:49-15:13	1	-60,60	5
7/23/2010	0559907,0222708	15:18-15:39	1	-50,50	4.2
1/28/2011	0560698,0221214	18:16-18:17	1.2	-60,60	5
1/28/2011	0560698,0221214	18:19-18:20	1.2	-60,60	5
1/28/2011	0560698,0221214	18:22-18:29	1.2	-60,60	5
1/28/2011	0560698,0221214	18:34-18:37	1.2	-60,60	5
1/28/2011	0560698,0221214	19:33-19:35	1.2	-60,60	5
1/28/2011	0560698,0221214	19:50-19:52	1.2	-60,60	5

### 3.1.2 NOVAC Version I Mini-DOAS

The NOVAC system is based on an Ocean Optics S2000 spectrometer that employs a linear silicon CCD array that recovers a spectrum from 280 to 420 nm. This is connected to the scanner unit, which consists of a mirror that scans 180° and is controlled electronically by the operating software, and a telescope with a quartz lens that defines a field of view of 8 mrad (Galle et al., 2010). The instrument is located at the coordinates 10.013526°, -83.784457°, and it is set to collect spectra in angular increments of 3.6° with an integration period of 3 seconds. The instrument is part of a global network that collects and stores volcanic SO<sub>2</sub> spectra from active volcanoes worldwide which are available online through the NOVAC project database (Galle et al., 2010). Time ranges for the data used in this analysis are shown in Table 5.

**Table 5:** Time ranges per day for analyzed data from the NOVAC database

<b>Date</b>	<b>Time Range (UTC)</b>
4/23/2010	11:56-19:11
4/28/2010	11:43-19:41
5/18/2010	12:13-19:21
5/30/2010	11:40-19:34
6/10/2010	11:39-19:13
8/13/2010	12:13-15:08

## 3.2 Mini-DOAS Data Analysis

### 3.2.1 MTU Resonance Mini-DOAS

The collected data were processed in order to estimate SO<sub>2</sub> emission rates using the same techniques used for COSPEC data analysis (William-Jones et al., 2008), which are explained below:



- 1) The width (in meters) of a horizontal cylindrical plume ( $d$ ) was determined using geometric calculations for two cases: with the plume nearly overhead and with the plume directly overhead (Figure 12). The height of the plume ( $a$ ) was assumed to be the same as the summit elevation of Turrialba). Measurements made with the mini-DOAS provided information such as the angular extent of the plume (Angle  $\beta$ ) and the elevation angle of the highest measured  $\text{SO}_2$  column (angle  $A$ ), which was assumed to be the plume center, which were used to calculate the distance ( $c$ ) from the plume center to the instrument (Applying Pythagoras' theorem using the angle  $A$ ).

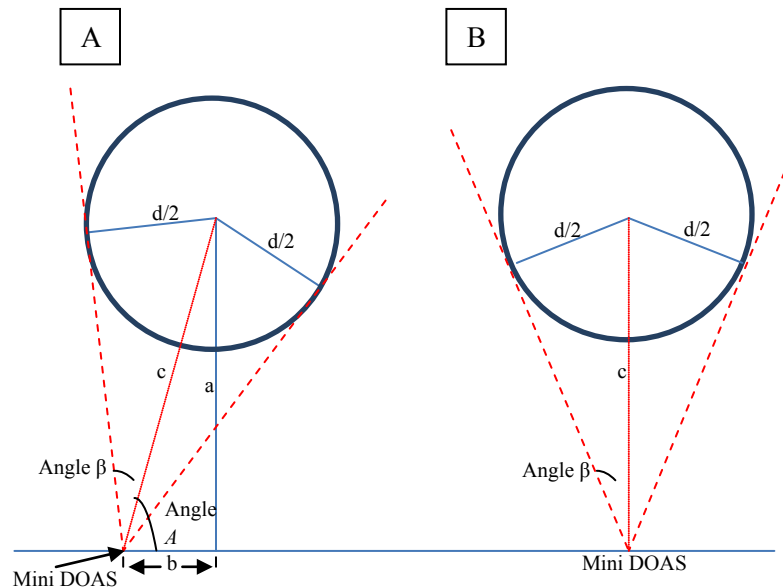


**Figure 12:** Methods to determine the plume width when nearly above (A), and when directly above (B). Reproduced from William-Jones et al. (2008) with permission of ©IAVCEI.

- 2) The plume  $\text{SO}_2$  columns were measured with the mini-DOAS and used to obtain the average column amount per transect (in units of ppm x m)

- 3) The plume speed was assumed to be the same as the hourly average wind speed (m/s) at the time of data collection, which was obtained from NOAA's READY archived meteorology database.
- 4) The SO<sub>2</sub> plume cross-section was determined from the product of the average column amount and the plume width (ppm x m<sup>2</sup>).
- 5) The SO<sub>2</sub> emission rate was calculated from the product of the SO<sub>2</sub> plume cross section and the plume speed (ppm x m<sup>3</sup> x s<sup>-1</sup>), and converted into tons per day (See Table 6).

**Table 6:** SO<sub>2</sub> fluxes obtained during mini-DOAS field deployment at Turrialba volcano

Date	Time Range (UTC)	SO <sub>2</sub> Flux (t/d)	Wind Speed (m/s)
7/23/2010	14:46:38-14:47:25	1058	5
7/23/2010	14:50:04-14:51:26	1015	5
7/23/2010	14:51:43-14:53:02	1208	5
7/23/2010	14:53:12-14:54:38	955	5
7/23/2010	14:54:40-14:56:14	1171	5
7/23/2010	15:01:39-15:02:38	1165	5
7/23/2010	15:02:55-15:04:14	1030	5
1/28/2011	18:16:25-18:17:01	1268	8.5
1/28/2011	18:19:45-18:20:20	1416	8.5
1/28/2011	18:22:36-18:23:11	966	8.5
1/28/2011	18:23:23-18:23:56	975	8.5
1/28/2011	18:24:11-18:24:46	902	8.5
1/28/2011	18:24:59-18:25:35	1336	8.5
1/28/2011	18:25:47-18:26:23	1090	8.5
1/28/2011	18:26:36-18:27:10	1541	8.5
1/28/2011	18:27:23-18:28:00	1141	8.5
1/28/2011	18:28:11-18:28:48	1420	8.5
1/28/2011	18:34:55-18:35:32	1136	8.5
1/28/2011	18:35:46-18:36:20	1256	8.5
1/28/2011	18:36:31-18:37:08	2442	8.5
1/28/2011	19:50:30-19:51:18	1264	8.5
1/28/2011	19:51:20-19:52:06	1483	8.5
1/28/2011	19:52:08-19:52:55	1304	8.5

### *3.2.2 NOVAC Mini-DOAS*

Spectral data collected by NOVAC's Mini-DOAS instruments are stored in their database and processed with the NOVAC software. Using wind speed data provided by the National Meteorological Institute of Costa Rica (IMN), assuming a plume height similar to the elevation of the crater, and obtaining the wind direction (calculated using triangulation methods), SO<sub>2</sub> emission rates for Turrialba were obtained and provided to us (Galle et al., 2010) (See Appendix C).

## **3.3 OMI Data Analysis**

Since OMI volcanic SO<sub>2</sub> burdens are essentially instantaneous measurements available once per day they do not provide direct estimations of SO<sub>2</sub> emission rates. Hence, in order to compare OMI measurements with SO<sub>2</sub> emission rates measured during ground-based mini-DOAS deployments, a technique to derive SO<sub>2</sub> emission rates from OMI SO<sub>2</sub> VCD data is required. We have explored several approaches to this, which are described below.

### *3.3.1 MODIS Smoke Estimation Technique*

In a study by Ichoku and Kaufman (2005), smoke emission rates from forest fires were estimated using data collected by the Moderate-Resolution Imaging Spectroradiometer (MODIS) sensor aboard the Terra and Aqua satellites. For each MODIS pixel within the area under analysis, Ichoku and Kaufman (2005) estimated smoke aerosol column mass densities, obtained wind speed data, and measured the length

of the smoke plume within the pixels (L). All the pixels covering the area containing smoke aerosols were clustered, and smoke emission rates were calculated by dividing the total mass of smoke aerosols by the average time period of emission of the smoke for all pixels. The latter is obtained by dividing L by the wind speed.

We adopt the Ichoku and Kaufman (2005) method using the OMI TRL SO<sub>2</sub> VCDs generated with the operational LF algorithm to estimate SO<sub>2</sub> emissions from Turrialba volcano. Wind speed data were obtained from NOAA's READY archived meteorology database and used to track how far from the volcano the SO<sub>2</sub> plume would have traveled, which OMI pixels the plume would have intersected and the time range required to traverse each OMI pixel. Since READY gives a range of wind speeds, we used the minimum, average, and maximum reported wind speeds for this analysis. We averaged the OMI SO<sub>2</sub> fluxes obtained for each wind speed and used the different time ranges obtained from the analysis to average the SO<sub>2</sub> fluxes and wind speeds derived from NOVAC's Mini-DOAS for each time range. The NOVAC data whose average wind speed was closest to the OMI data for a given time range was used for the comparison of SO<sub>2</sub> emission rates.

SO<sub>2</sub> fluxes were estimated from individual OMI pixels using the following equation:

$$\text{SO}_2 \phi = Mv/L \quad (6)$$

where SO<sub>2</sub>  $\phi$  is the emission rate (kt/s), M is the SO<sub>2</sub> mass in the pixel (kt), v is the wind speed (m/s), and L is the length of the SO<sub>2</sub> plume through the pixel (m). In order to

estimate the minimum SO<sub>2</sub> emission rate through a pixel, a diagonal line from the two opposite corners of each pixel was used to measure the maximum length of the volcanic plume assuming the wind blows continuously and linearly (See Appendix D). The days that were analyzed were chosen according to the following criteria: a) the OMI overpass coincided with days on which several hours of ground-based mini-DOAS measurements were available in order to compare the results, b) the satellite was at or near-nadir, providing optimal spatial resolution, c) the volcanic SO<sub>2</sub> plume was partly/completely visible in the OMI image since clouds often obscure the plume, and d) Turrialba volcano was the dominant source of volcanic SO<sub>2</sub> for the analyzed pixels.

### *3.3.2 OMI SO<sub>2</sub> Lifetime Technique*

OMI volcanic SO<sub>2</sub> burdens are not directly representative of volcanic SO<sub>2</sub> emission rates, but they can be used to estimate emission rates if the SO<sub>2</sub> lifetime in the atmosphere is known. The OMI TRL SO<sub>2</sub> maps generated with the LF algorithm for Turrialba volcano were further analyzed in order to determine the lifetime of SO<sub>2</sub> for the days under analysis. Daily wind speed (m/s) data were obtained from NOAA's READY archived meteorology database and used to calculate a daily average wind speed value for the volcanic plume. Assuming a constant wind speed and direction, the lifetime ( $\tau$ ) of volcanic SO<sub>2</sub> from Turrialba was estimated for each daily image under analysis using the same procedures for equations 3, and 4 in Section 2.2.3 (See Figure 13). Using the SO<sub>2</sub> mass burdens (M) obtained using the NCM technique for the days under analysis and the

calculated  $\text{SO}_2$  lifetime for the area under analysis,  $\text{SO}_2$  emission rates were estimated using equation 5.

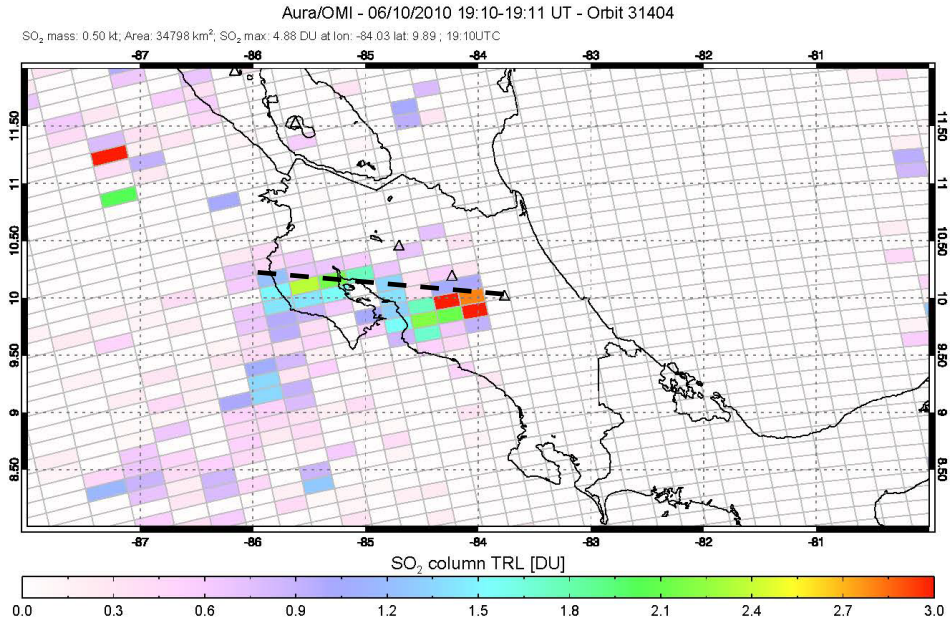


**Figure 13:** Example of a daily OMI  $\text{SO}_2$  image where the black dashed line represents the volcanic plume trajectory with a constant wind direction.

OMI images illustrate variations in wind direction by observing the drift of the volcanic plume captured at the time of the satellite overpass. Further analysis was performed using the same calculations as described above, but assuming a variable wind direction with a constant speed (Figure 14). We approximated the trajectory of the plume by choosing the OMI pixels with higher VCDs within the plume, measured the distance between these pixels, and summed them to obtain the total distance traveled by the plume.

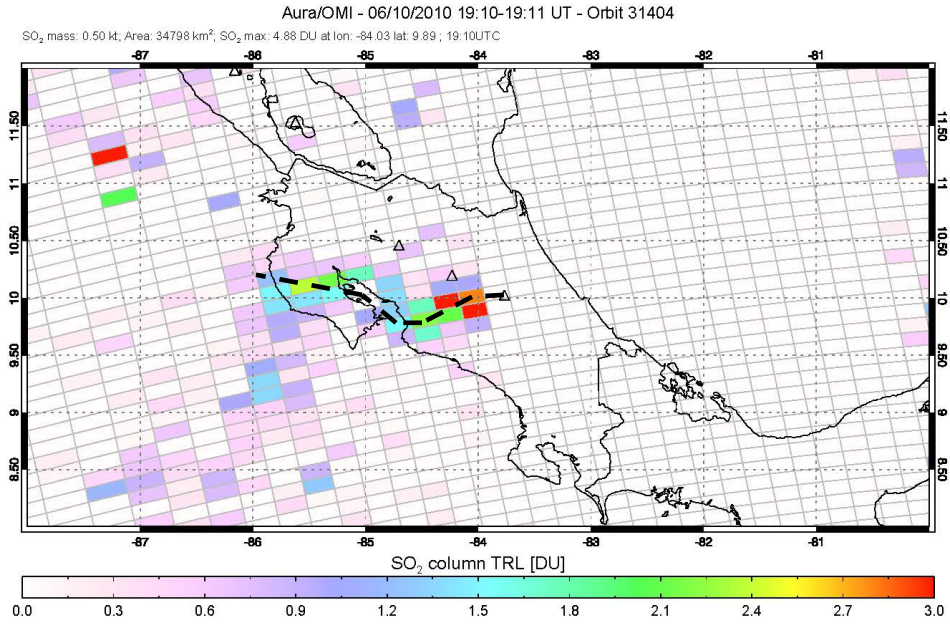


**Figure 14:** Example of a daily OMI SO<sub>2</sub> image where the black dashed line represents the volcanic plume trajectory with a variable wind direction.

### 3.3.3 OMI SO<sub>2</sub> Transects Technique

The newest version of the OMIPLOT software can automatically calculate SO<sub>2</sub> emission rates (t/d) using transects across the SO<sub>2</sub> plume measured by OMI (unpublished version by Simon Carn 2011). The procedure is essentially the same as that used to process COSPEC and mini-DOAS traverse measurements, and requires an estimate of the plume speed (i.e., wind speed). Days on which near-coincident OMI and mini-DOAS data for Turrialba's volcanic plume were available were chosen for this analysis. After generating LF gridded plots of OMI SO<sub>2</sub> data for the selected days, transects were drawn across Turrialba's SO<sub>2</sub> plume perpendicular to the apparent plume transport direction (Figure 15). The software automatically calculates the plume width and average SO<sub>2</sub> column in the cross-section, and uses this information and a wind speed input by the user

to calculate  $\text{SO}_2$  emission rates (t/d) for the different  $\text{SO}_2$  CMAs assumed in the LF retrieval algorithm.

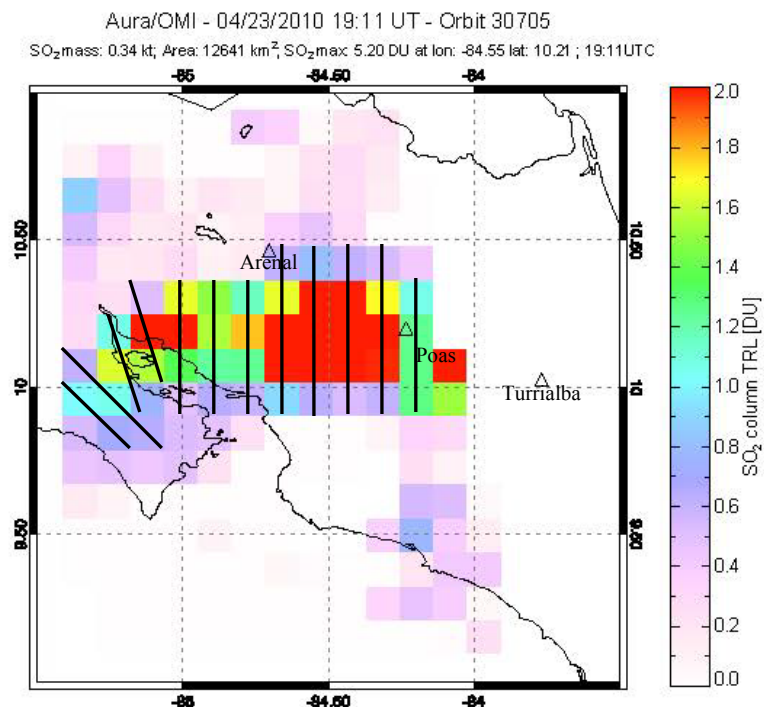


**Figure 15 A:** April 23, 2010 OMI  $\text{SO}_2$  map used for  $\text{SO}_2$  emission rate estimation using the plume transect technique. The  $\text{SO}_2$  plume transects used are indicated by the black near-parallel lines along the volcanic plume.



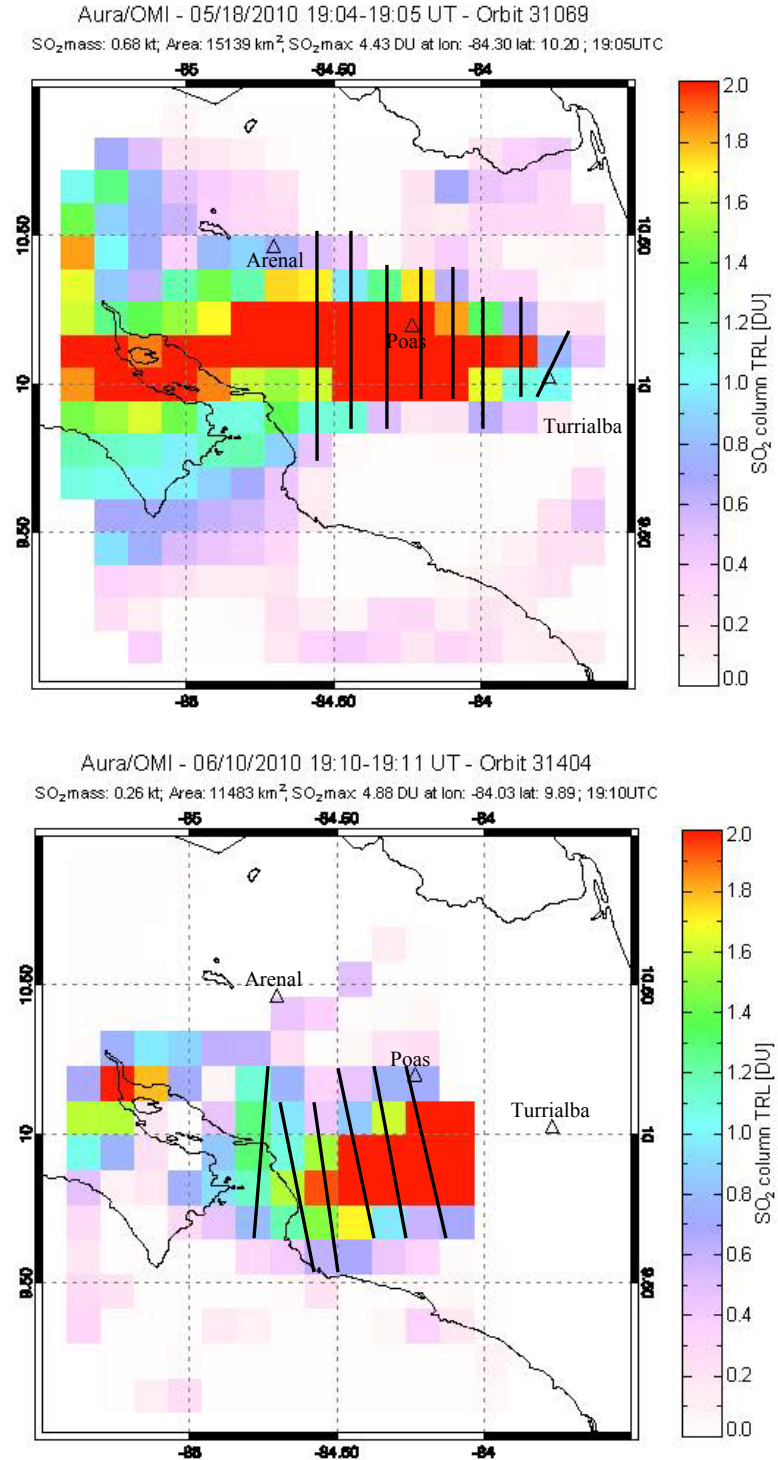


**Figure 15 B:** May 18, and June 10, 2010 OMI  $\text{SO}_2$  maps used for  $\text{SO}_2$  emission rate estimation using the plume transect technique. The  $\text{SO}_2$  plume transects used are indicated by the black near-parallel lines along the volcanic plume.

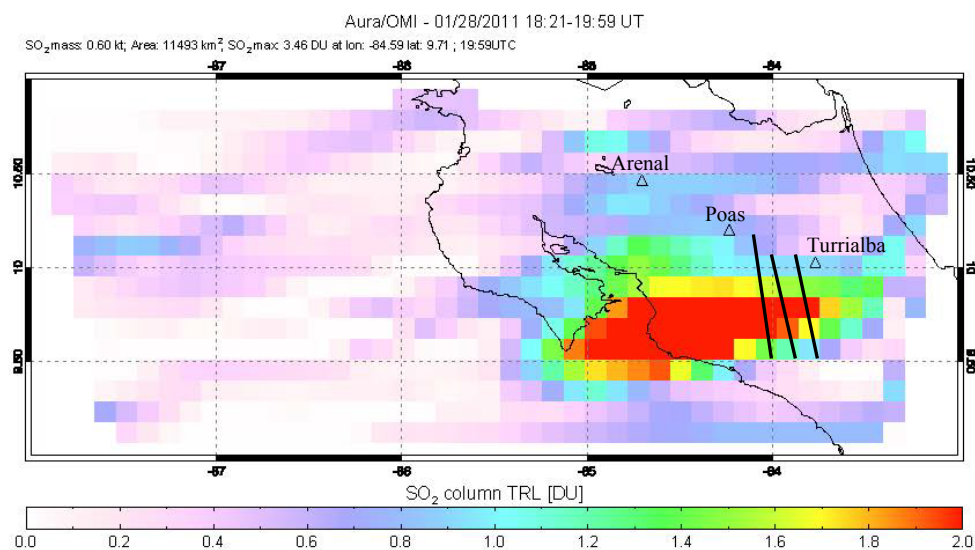
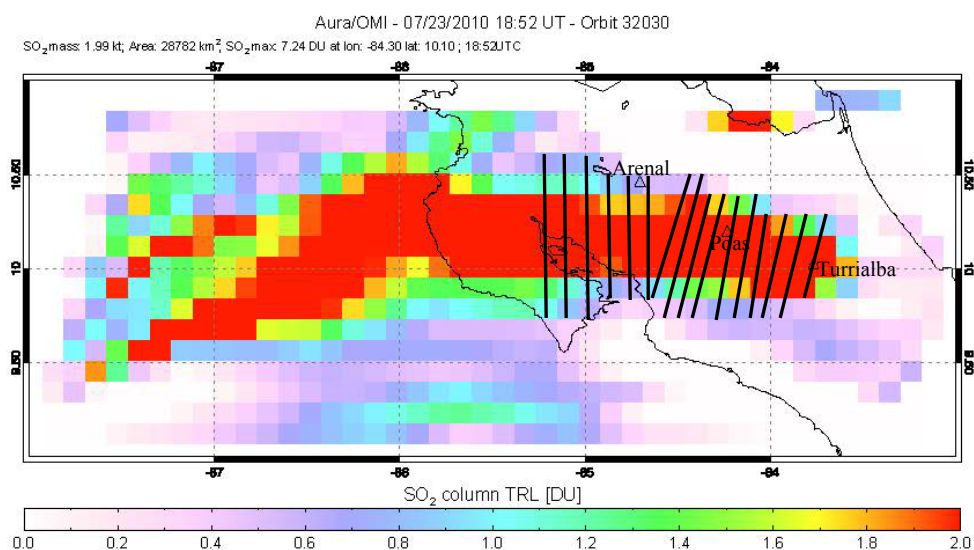


**Figure 15 C:** July 23, 2010, and January 28, 2011 OMI SO<sub>2</sub> maps used for SO<sub>2</sub> emission rate estimation using the plume transect technique. The SO<sub>2</sub> plume transects used are indicated by the black near-parallel lines along the volcanic plume.

### 3.4 Comparisons between OMI and Mini-DOAS

#### *3.4.1 MODIS Smoke Estimation Technique*

Table 7 shows the SO<sub>2</sub> fluxes obtained using this technique for the analyzed days. Data from May 30 and August 13 seemed to be in good agreement with the NOVAC data with a percentage difference of 7.2% and -4.3%, while that from April 28, May 18 and June 10 have a percentage difference of -84.2%, -49.6%, and -68.13% respectively. As mentioned above, estimating SO<sub>2</sub> emissions from satellite measurements on days where there is significant cloud coverage increases the error on the results, which is difficult to evade at Turrialba due to its tropical climate. OMI-derived cloud fractions, reflectivity, and cloud top pressure for the pixels under analysis were obtained, although their relationship to the fluxes was difficult to interpret (Table 7). In order to have a better understanding of the relationship between these results, further information is needed on the location of the SO<sub>2</sub> plume with respect to the clouds (below, mixed, or above the clouds) at the time of data collection and at the time of the OMI overpass. For this reason, we used the cloud top pressure to estimate the cloud height for each pixel and made interpretations with some assumptions.

Data from April 28 and May 18 were obtained for a day with high cloud coverage and clouds that were over the 3 km volcanic plume, which may cause underestimation of OMI SO<sub>2</sub> VCD data as compared to the NOVAC measurements. Data from May 30 and August 13 showed an agreement between the instruments but the results suggest that both instruments underestimated the SO<sub>2</sub> VCD. High cloud coverage and clouds that are located over (May 30) and mixed (August 13) within the 3 km volcanic plume may have

caused underestimation of OMI SO<sub>2</sub> VCD data. Since the NOVAC data measured similar SO<sub>2</sub> fluxes as those obtained from OMI data, it might indicate that clouds were either mixed within the plume or located above the plume at the time of the ground-based measurements, which would result in an underestimation of SO<sub>2</sub>. Data from June 10 was obtained with high cloud coverage and clouds that were mixed within the 3 km volcanic plume that may have caused underestimation of OMI SO<sub>2</sub> VCD data (Table 7).

Surface reflectivity assists in the detection of small SO<sub>2</sub> plumes but as well can produce overestimations of SO<sub>2</sub> in cases where the air mass factor (ratio between retrieved slant column and the atmospheric vertical column of the absorber) needs to be adjusted (Krotkov et al., 2006). The days under analysis had high reflectivity values but did not result in an overestimation of the obtained OMI SO<sub>2</sub> flux, suggesting that the air mass factor was well adjusted and that it was not directly affecting the SO<sub>2</sub> retrievals for the analyzed days (Table 7)

**Table 7:** SO<sub>2</sub> fluxes obtained from OMI using the MODIS Smoke Emission Technique, and by averaging the results from the NOVAC Project Database

Date	OMI SO <sub>2</sub> Flux (t/d)	NOVAC SO <sub>2</sub> Flux (t/d)	Pixel number	OMI Pixel Cloud Fraction (Average)	OMI Pixel Reflectivity (%)	OMI Pixel Cloud Top Pressure (mb)	Cloud Height (km) Approximation from U.S. Standard Atmosphere, 1976
4/28/2010	99	628	1	0.95	73	485	5-6
5/18/2010	365	724	2	0.55	36	409	7-8
5/30/2010	463	432	2	0.63	44	592	4-5
6/10/2010	232	728	1	0.76	51	628	3-4
			2	0.54	35	634	3-4
			3	0.20	21	923	0-1
8/13/2010	353	369	1	1.000	80	633	3-4

Another factor to consider when calculating SO<sub>2</sub> emissions with this technique is the spatial resolution of the OMI images. The smoke emission analysis (Ichoku and Kaufman, 2005) used MODIS aerosol pixels that measure 10 x 10 km at nadir, whereas OMI pixels measure 13 x 24 km at nadir. The mass per pixel retrieved by OMI is averaged over a larger area and therefore SO<sub>2</sub> flux calculations with this technique are expected to be less accurate relative to data from a higher resolution instrument, particularly for volcanic plumes much smaller than the OMI pixel size. This technique is therefore problematic for the calculation of accurate SO<sub>2</sub> emission rates for small volcanic plumes due to the spatial resolution of the instrument and because of the lack in understanding from the effects of different atmospheric conditions, and consequently for OMI satellite validation in such cases. However, it is useful for estimating SO<sub>2</sub> fluxes from single pixels on days when there are data gaps over Turrialba where parts of the plume are still visible.

#### *3.4.2 OMI SO<sub>2</sub> Lifetime Technique*

Tables 8 and 9 show the SO<sub>2</sub> lifetime and flux estimations calculated under the specified conditions. The estimated volcanic SO<sub>2</sub> lifetimes for a plume that varied in transportation direction showed an average of 9.3% increase relative to that with a constant wind direction. This resulted in an average 8.2% decrease in the SO<sub>2</sub> fluxes estimated using a varying wind direction. As observed in the daily OMI images, the drifting volcanic plume shows a variation in wind transport direction. For this reason, the

SO<sub>2</sub> fluxes obtained with a varying plume direction were used for comparisons with fluxes obtained using the Mini-DOAS.

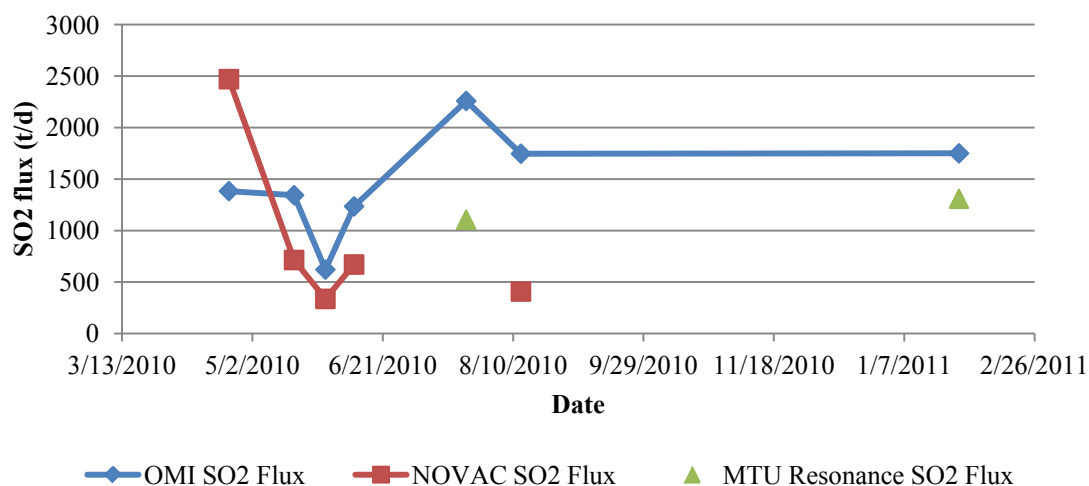
Figure 16 illustrates a similar pattern, indicating a good agreement between the ground-based and satellite-based measurements and therefore an initial qualitative validation of the OMI data. The differences in the magnitude of the SO<sub>2</sub> fluxes could be due to various reasons. The main source of error is the wind data since we assumed a constant wind speed and a continuous wind direction, which are unlikely to represent the true wind characteristics. As shown in Tables 8 and 9, using a variable wind direction for the calculations gives a higher SO<sub>2</sub> lifetime and therefore a lower SO<sub>2</sub> emission rate. Future algorithms could reduce this error by including wind dispersion modeling along with wind speed data to provide a more accurate plume trajectory and estimation of the SO<sub>2</sub> lifetime. Uncertainties in the plume height used for the calculations are also a source of error since for the ground measurements we assumed a plume height equal to Turrialba's summit elevation. However, SO<sub>2</sub> plumes from Turrialba occasionally rising up to 2 km above the summit have been reported (Simkin and Siebert, 2002-2011b).

**Table 8:** Turrialba's volcanic SO<sub>2</sub> lifetime and fluxes under constant wind direction

Date	Distance traveled per day (km)	Direct distance from volcano to furthest point of plume (km)	Lifetime SO <sub>2</sub> (days)	OMI SO <sub>2</sub> Flux (tons/day)
4/23/2010	830	455	0.55	1426
5/18/2010	182	325	1.35	1531
5/30/2010	134	155	1.15	717
6/10/2010	504	275	0.55	1360
7/23/2010	432	430	1	2353
8/13/2010	470	213	0.45	1779
1/28/2011	634	173	0.27	2094

**Table 9:** Turrialba's volcanic SO<sub>2</sub> lifetime and fluxes under varying wind directions

Date	Distance traveled per day (km)	Distance with varying plume direction (km)	Lifetime SO <sub>2</sub> (days)	OMI SO <sub>2</sub> Flux (tons/day)
4/23/2010	830	469	0.56	1383
5/18/2010	182	402	1.54	1344
5/30/2010	134	179	1.33	621
6/10/2010	504	303	0.60	1235
7/23/2010	432	448	1.04	2259
8/13/2010	470	217	0.46	1746
1/28/2011	634	207	0.33	1750

**Figure 16:** Comparisons between OMI data and Mini DOAS measurements under varying wind conditions

### 3.4.3 OMI SO<sub>2</sub> Transects Technique

Three days of data obtained by NOVAC's Mini-DOAS and the two days of field deployment with the Resonance Mini-DOAS were used for comparisons with the OMI transects (Appendix E). Using wind speed data from READY for the days on which measurements were taken with the Resonance Mini-DOAS and the wind speeds used to

calculate NOVAC SO<sub>2</sub> fluxes, we determined the location within the OMI transects that coincided with the time range when ground-based measurements were obtained.

Data collected on April 23 are presented in Table 10 and plotted in Figure 17. The most accurate SO<sub>2</sub> fluxes calculated using the transect technique were those located closest to the volcanic source (transects 1 and 2 which were measured 49 and 62 km from the main vent due to a data gap over Turrialba). Nonetheless, OMI SO<sub>2</sub> fluxes might be erroneous if transects are drawn too close to the volcano because the volcanic plume would not have dispersed enough to cover sufficient fraction of the large OMI pixels, resulting in the underestimation of SO<sub>2</sub>. OMI SO<sub>2</sub> fluxes were less accurate at greater distances from the volcanic source, with the exception of transects 10 and 11 that coincide with the minimum fluxes obtained by the NOVAC instrument. These observations support the fact that as the plume ages the SO<sub>2</sub> concentration is reduced due to atmospheric dispersion and chemical processing and could be used in the future along with other sources of information to estimate the SO<sub>2</sub> loss rate under varying atmospheric conditions. This information is needed to produce results that are more representative of the total volcanic emissions rather than depleted volcanic SO<sub>2</sub> concentrations which result in an underestimation of the volcanic input into the troposphere.

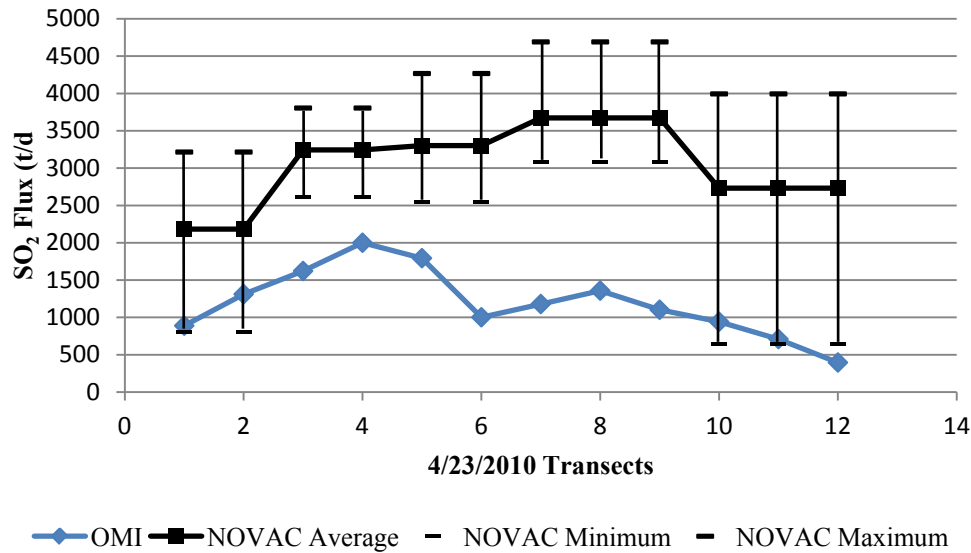
Data collected on May 18 are presented in Table 11 and plotted in Figure 18. The most accurate OMI-derived SO<sub>2</sub> fluxes were derived from transects 5, 6, and 7, which were measured 52 km, 64 km, and 76 km from the main vent, respectively. These distances overlap with those measured for the April 23 data described above. However, wind speed measurements differed on the two days analyzed, and the cloud fraction at the time of the OMI overpass was higher on April 23, which suggests that clouds could have



increased the rate of SO<sub>2</sub> depletion via aqueous phase reactions. Furthermore, this process might be accelerated within this particular distance range due to changes in the topography (from higher to lower elevations), increasing the temperature and pressure at lower elevations and therefore creating a more oxidizing environment.

**Table 10:** SO<sub>2</sub> fluxes obtained by the Mini-DOAS and OMI transects on 4/23/2010

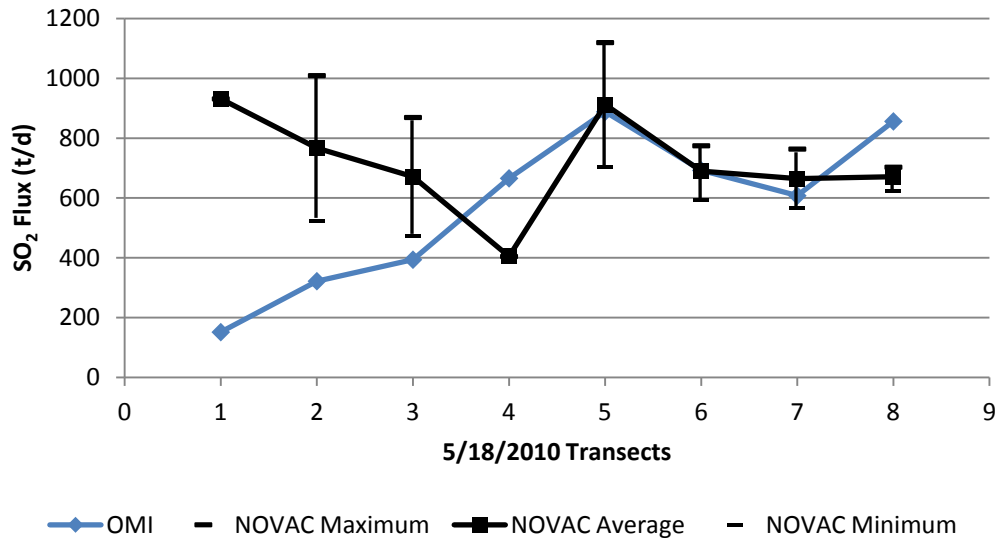
4/23/2010	NOVAC Average SO <sub>2</sub> Flux (t/d)	NOVAC Minimum SO <sub>2</sub> Flux (t/d)	NOVAC Maximum SO <sub>2</sub> Flux (t/d)	3km OMI SO <sub>2</sub> Flux (t/d)
Transects 1, 2	2184	810	3214	888 (1) 1311 (2)
Transects 3, 4	3244	2607	3804	1621 (3) 2000 (4)
Transects 5, 6	3301	2539	4266	1793 (5) 1001 (6)
Transects 7, 8, 9	3672	3087	4690	1179 (7) 1358 (8) 1102 (9)
Transects 10, 11, 12	2732	647	3993	942 (10) 709 (11) 395 (12)



**Figure 17:** OMI SO<sub>2</sub> fluxes measured from plume transects compared to SO<sub>2</sub> fluxes obtained by the Mini-DOAS on April 23, 2010. The minimum and maximum SO<sub>2</sub> fluxes obtained by NOVAC are also plotted to visualize the range of obtained measurements.

**Table 11:** SO<sub>2</sub> fluxes obtained by the Mini-DOAS and OMI transects during 5/18/2010

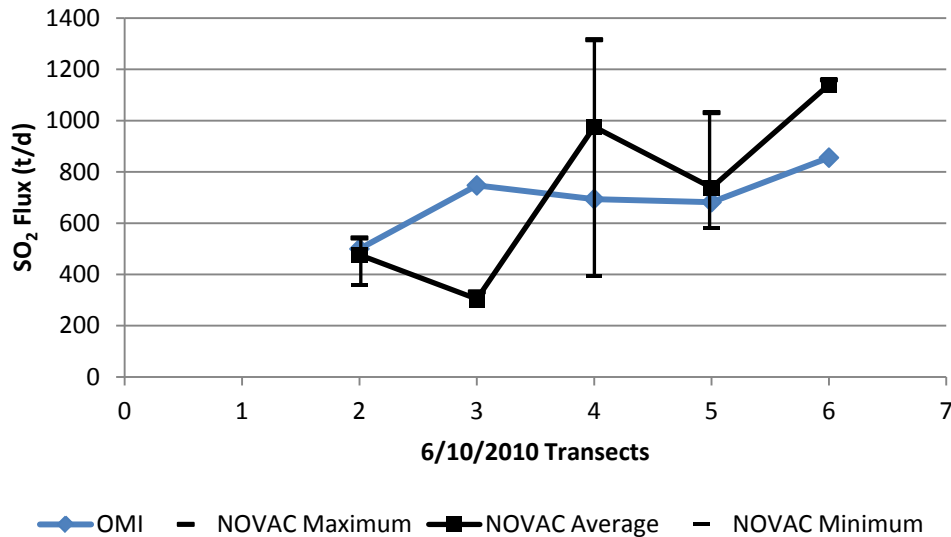
5/18/2010	NOVAC Average SO <sub>2</sub> Flux	NOVAC Minimum SO <sub>2</sub> Flux	NOVAC Maximum SO <sub>2</sub> Flux	3km OMI SO <sub>2</sub> Flux (t/d)
Transect 1	932	932	932	152
Transect 2	767	524	1009	322
Transect 3	671	472	869	394
Transect 4	405	405	405	666
Transect 5	912	705	1120	888
Transect 6	690	593	775	692
Transect 7	664	565	764	608
Transect 8	671	623	703	856

**Figure 18:** OMI SO<sub>2</sub> fluxes measured from plume transects compared to SO<sub>2</sub> fluxes obtained by the Mini-DOAS on May 18, 2010. The minimum and maximum SO<sub>2</sub> fluxes obtained by NOVAC are also plotted to visualize the range of obtained measurements.

Data collected on June 10 are presented in Table 12 and plotted in Figure 19. The transects obtained on this day were quite accurate with the exception of transect 3 and 6. There was a high cloud fraction in the area on this day and if the plume was located above the clouds at the time of Mini-DOAS measurements it could account for the higher SO<sub>2</sub> flux measured by OMI relative to the Mini-DOAS. On the other hand, transect 6 was located 114 km from the main vent by which time significant SO<sub>2</sub> depletion would be expected, accounting for the difference in SO<sub>2</sub> fluxes.

**Table 12:** SO<sub>2</sub> fluxes obtained by the Mini-DOAS and OMI transects during 6/10/2010

6/10/2010	NOVAC Average SO <sub>2</sub> Flux	NOVAC Minimum SO <sub>2</sub> Flux	NOVAC Maximum SO <sub>2</sub> Flux	OMI SO <sub>2</sub> Flux (3 km)
Transect 2	476	357	542	499
Transect 3	304	277	332	747
Transect 4	976	392	1316	694
Transect 5	739	581	1031	682
Transect 6	1140	1121	1159	855

**Figure 19:** OMI SO<sub>2</sub> fluxes measured from plume transects compared to SO<sub>2</sub> fluxes obtained by the Mini-DOAS on June 10, 2010. The minimum and maximum SO<sub>2</sub> fluxes obtained by NOVAC are also plotted to visualize the range of obtained measurements.

The July 23 mini-DOAS data coincide with OMI transects 7 and 8 (Figure 15); these results are presented in Table 13. This data were obtained under favorable conditions for OMI validation since at the time of ground-based measurements there was a cloud-free background, the satellite was near nadir (with a pixel dimension of ~50 km), and there was a constant wind speed of 5 m/s during the entire day. However, the results showed a disagreement, with OMI estimations being ~250% larger. There are various errors that could account for such a discrepancy. The Mini-DOAS data for this day were obtained early in the morning which is when the background noise is higher and can give

an error of ~20% (Edmonds et al., 2003a). There is also the error associated with the wind speed measurements since we assumed a constant wind speed for the entire day according to the data obtained from READY. Furthermore, at the time of field measurements the wind was easterly, but it is apparent in the OMI image that the plume transport direction was not constant throughout the day. This may cause the plume to appear wider than its actual width if parcels of SO<sub>2</sub> separate from the main air mass flow and travel at different speeds, creating a layered plume and the low spatial resolution resulting in an overestimation of SO<sub>2</sub> in OMI.

OMI retrievals can obtain SO<sub>2</sub> VCD overestimations in the presence of highly reflective clouds at the time of the OMI overpass. This is clearly seen in Figure 20, which is an OMI image plotted over an image taken by NASA's Aqua satellite, which has an overpass just minutes before the Aura satellite (<http://atrain.nasa.gov/>). In the image, highly reflective clouds are causing OMI to detect an SO<sub>2</sub> signal in areas where there are no sources of SO<sub>2</sub>, suggesting that OMI might be overestimating SO<sub>2</sub> in the volcanic plume for this particular day.

The January 28 data were tracked to be located between transects 1, 2, and 3 (See Table 14). This particular data set is not the best for attempting validation of OMI, mainly because the satellite was not near nadir, with analyzed pixels measuring 14 x 117 km<sup>2</sup>. However, the results showed an agreement, falling completely between the ranges obtained by the Mini-DOAS measurements.

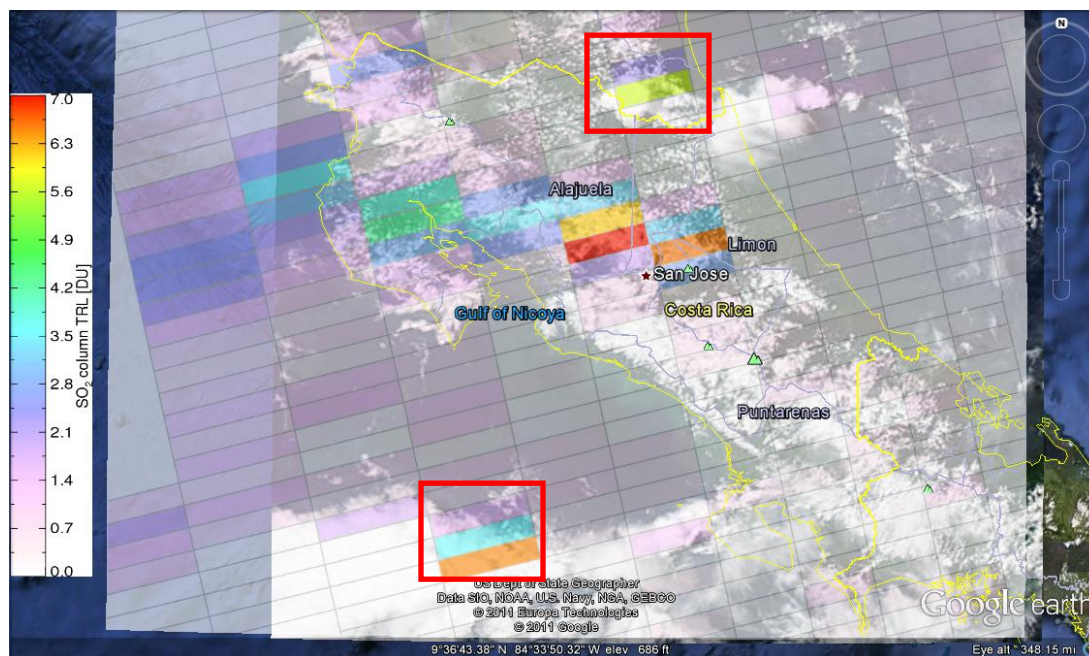


**Figure 20:** July 23, 2010 OMI image over the Aqua satellite image ([http://lance-modis.eosdis.nasa.gov/imagery/subsets/?subset=SERVIR\\_CostaRica.2010204.aqua.1km](http://lance-modis.eosdis.nasa.gov/imagery/subsets/?subset=SERVIR_CostaRica.2010204.aqua.1km)) . Red boxes enclose two areas without an SO<sub>2</sub> source that are measuring high SO<sub>2</sub> concentrations due to highly reflective clouds.

**Table 13:** SO<sub>2</sub> fluxes obtained by the Mini-DOAS and OMI transects on 7/23/2010

7/23/2010	Resonance Average SO <sub>2</sub> Flux	Resonance Minimum SO <sub>2</sub> Flux	Resonance Maximum SO <sub>2</sub> Flux	OMI SO <sub>2</sub> Flux (3 km)
Transect 7,8	1106	955	1208	2766 2745

**Table 14:** SO<sub>2</sub> fluxes obtained by the Mini-DOAS and OMI transects during 1/28/2011

1/28/2011	Resonance Average SO <sub>2</sub> Flux	Resonance Minimum SO <sub>2</sub> Flux	Resonance Maximum SO <sub>2</sub> Flux	OMI SO <sub>2</sub> Flux (3 km)
Transect 1,2,3	1309	902	2442	1516 1703 2010

## 4. Conclusions

We have evaluated two new OMI retrieval analysis techniques and determined that the NCM technique provides a better estimation of the SO<sub>2</sub> burden for Turrialba volcano. Nonetheless, the BRI technique provides results with a general agreement of 91% and high correlation factors with the NCM. This comparison demonstrates that the automatic operational OMI SO<sub>2</sub> mass calculation provides accurate estimations of volcanic SO<sub>2</sub> burdens in the lower troposphere when: a) nearby volcanoes are not emitting SO<sub>2</sub>; b) cloud coverage is minimal (less accurate results during the wet season); c) clouds are located below the volcanic plume. Further improvements should be made to have a better understanding of the lifetime and depletion rates of volcanic SO<sub>2</sub> under different atmospheric conditions in order to have a better estimation of the undepleted SO<sub>2</sub> emitted by the volcano for accurate volcano monitoring applications. Parameters for the automatic OMI retrieval of volcanic SO<sub>2</sub> should also be revised in order to obtain better VCD measurements under cloudy conditions. Improvements on automatic OMI retrievals of volcanic SO<sub>2</sub> could be achieved by using other wavelengths where there is less absorption from clouds in order to obtain better pair residual estimations and by decreasing the analysis region for minimum background noise input.

Comparisons between SO<sub>2</sub> emission rates obtained using different OMI analysis techniques and the Mini DOAS gave variable results. The MODIS smoke estimation technique proved to be inaccurate for the estimation of emission rates with OMI, mainly due to the spatial resolution of the instrument and the underestimations produced by the atmospheric conditions; still it could be useful to obtain SO<sub>2</sub> flux measurements on days

when data gaps are present. The OMI SO<sub>2</sub> lifetime technique provided qualitative agreement between the ground-based and satellite-based data. This technique benefits from reduced noise due to averaging over a larger area, supporting potential development of automatic computing applications in the near future. The OMI transect technique provided occasional quantitative agreements with the Mini-DOAS measurements during the days under analysis. These results provide some further validation of the OMI volcanic SO<sub>2</sub> retrievals and prove this technique to be a promising method for accurate and precise calculations of SO<sub>2</sub> emission rates under specific atmospheric conditions which should be furthered studied in order to implement it for volcano monitoring.

#### **4.1 Future Work**

An error analysis should be made for each of the OMI analysis techniques in order to determine the degree of uncertainty from the results. Further studies are recommended with new techniques that evaluate Turrialba's volcanic SO<sub>2</sub> data under unfavorable conditions since this tends to be the case for most days with the available instruments. Interpolation methods with OMI data should be analyzed in more detail since it seems to give reasonable estimations in particular for days when the satellite is not at/near nadir, as demonstrated by the accurate data obtained on January 28, 2011. Moreover, SO<sub>2</sub> loss rates are not constant throughout the volcanic plume and could be evaluated with OMI in the future using the OMIPLOT software, which supplies other information for each pixel under analysis (e.g., cloud fraction, reflectivity, aerosol index, and ozone column). These should be integrated with the SO<sub>2</sub> retrievals and further

analyzed in order to determine how they affect the volcanic SO<sub>2</sub> emissions through time using ground-based data for comparison.

Software that automatically obtains SO<sub>2</sub> burdens (such as the BRI) could use average wind speed and direction obtained from a meteorological database. The program could automatically select the most distant OMI volcanic SO<sub>2</sub> pixel with respect to the volcanic source, within the wind direction and plume area under analysis. It should determine the SO<sub>2</sub> lifetime depending on the wind speed and use it to calculate minimum daily emission rates, which could later be improved with better knowledge of the prevailing atmospheric conditions. For our wind data, we used the Global Data Assimilation System (GDAS) in NOAA's READY which consists of an operational computer analysis and forecast model, with the final product being a 3-hour forecast produced 4 times a day (0:00, 6:00, 12:00, and 18:00 UTC). A model that produces data more frequently is required to make more accurate estimates of SO<sub>2</sub> emission rates.



## 5. References

- Allard, P., 1997. Endogenous magma degassing and storage at Mount Etna. *Geophys. Res. Lett.*, 24(17): 2219-2222.
- Allard, P., Carbonnelle, J., Metrich, N., Loyer, H. and Zettwoog, P., 1994. Sulphur output and magma degassing budget of Stromboli volcano. *Nature*, 368(6469): 326-330.
- Alvarado, G.E., Carr, M.J., Turrin, B.D., Swisher, C.C., Schmincke, H.U. and Hudnut, K.W., 2006. Recent volcanic history of Irazu volcano, Costa Rica: Alternation and mixing of two magma batches, and pervasive mixing. In: W.I. Rose, G.J.S. Bluth, M.J. Carr, J.W. Ewert, L.C. Patino and J.W. Vallance (Editors), *Volcanic hazards in Central America*. Geological Society of America, Boulder, CO, pp. 259-276.
- Bellon, H. and Tournon, J., 1978. Contribution de la geochronometrie K-Ar a l'etude du magmatisme de Costa Rica, Amerique Centrale. *Bulletin de la Societe Geologique de France*, 7: 955-959.
- Bhartia, P.K. and Wellemeyer, C.W., 2002. TOMS-V8 Total Ozone Algorithm. In: P.K. Bhartia (Editor), *OMI Algorithm Theoretical Basis Document, OMI Ozone Products*. NASA Goddard Space Flight Center, Greenbelt, Maryland, USA, pp. 1-91.
- Bluth, G.J.S., Casadevall, T.J., Schnetzler, C.C., Doiron, S.D., Walter, L.S., Krueger, A.J. and Badruddin, M., 1994. Evaluation of sulfur dioxide emissions from explosive volcanism: the 1982–1983 eruptions of Galunggung, Java, Indonesia. *Journal of Volcanology and Geothermal Research*, 63(3-4): 243-256.
- Campion, R., Salerno, G.G., Coheur, P., Hurtmans, D., Clarisse, L., Kazahaya, K., Burton, M.R., Caltabiano, T., Clerbaux, C. and Bernard, A., 2010. Measuring volcanic degassing of SO<sub>2</sub> in the lower troposphere with ASTER band ratios. *Journal of Volcanology and Geothermal Research*, 194(1-3): 42-54.
- Carn, S.A., 2011. OMIPLOT. <http://vhub.org/resources/682>
- Carn, S.A., Froyd, K.D., Anderson, B.E., Wennberg, P., Crounse, J., Spencer, K., Dibb, J.E., Krotkov, N.A., Browell, E.V., Hair, J.W., Diskin, G., Sachse, G. and Vay, S.A., 2011. In situ measurements of tropospheric volcanic plumes in Ecuador and Colombia during TC4. *Journal of Geophysical Research*, 116(D00J24): 1-24.
- Carn, S.A., Krueger, A.J., Arellano, S., Krotkov, N.A. and Yang, K., 2008. Daily monitoring of Ecuadorian volcanic degassing from space. *Journal of Volcanology and Geothermal Research*, 176(1): 141-150.
- Carn, S.A., Krueger, A.J., Bluth, G.J.S., Schaefer, S.J., Krotkov, N.A., Watson, I.M. and Datta, S., 2003. Volcanic eruption detection by the Total Ozone Mapping Spectrometer (TOMS) instruments: a 22-year record of sulphur dioxide and ash emissions. Geological Society, London, Special Publications, 213(1): 177-202.

- Carn, S.A., Krueger, A.J., Krotkov, N.A., Yang, K. and Evans, K., 2009. Tracking volcanic sulfur dioxide clouds for aviation hazard mitigation. *Natural Hazards*, 51(2): 325-343.
- Casadevall, T.J., Johnston, D.A., Harris, D.M., Rose, W.I., Malinconico, L.L., Stoiber, R.E., Bornhorst, T.J., Williams, S.N., Woodruff, L. and Thompson, J.M., 1981. SO<sub>2</sub> emission rates at Mount St. Helens from March 29 through December, 1980. In: P.W. Lipman and D.R. Mullineaux (Editors), *The 1980 eruptions of Mount St. Helens, Washington*. United States Geological Survey, Washington, D.C., pp. 1-844.
- Charlson, R.J., Schwartz, S.E., Hales, J.M., Cess, R.D., Coakley, J.A., Hansen, J.E. and Hofmann, D.J., 1992. Climate Forcing by Anthropogenic Aerosols. *Science*, 255(5043): 423-430.
- Delmelle, P., 2003. Environmental impacts of tropospheric volcanic gas plumes. In: C. Oppenheimer, D.M. Pyle and J. Barclay (Editors), *Volcanic Degassing*. Geological Society, Bath, UK, pp. 381-400.
- Delmelle, P., Stix, J., Baxter, P., Garcia-Alvarez, J. and Barquero, J., 2002. Atmospheric dispersion, environmental effects and potential health hazard associated with the low-altitude gas plume of Masaya volcano, Nicaragua. *Bulletin of Volcanology*, 64(6): 423-434.
- Diaz, J.A., Pieri, D., Arkin, C.R., Gore, E., Griffin, T.P., Fladeland, M., Bland, G., Soto, C., Madrigal, Y., Castillo, D., Rojas, E. and Achí, S., 2010. Utilization of in situ airborne MS-based instrumentation for the study of gaseous emissions at active volcanoes. *International Journal of Mass Spectrometry*, 295(3): 105-112.
- Edmonds, M., Herd, R.A., Galle, B. and Oppenheimer, C.M., 2003a. Automated, high time-resolution measurements of SO<sub>2</sub> flux at Soufrière Hills Volcano, Montserrat. *Bulletin of Volcanology*, 65(8): 578-586.
- Edmonds, M., Oppenheimer, C., Pyle, D.M., Herd, R.A. and Thompson, G., 2003b. SO<sub>2</sub> emissions from Soufrière Hills Volcano and their relationship to conduit permeability, hydrothermal interaction and degassing regime. *Journal of Volcanology and Geothermal Research*, 124(1-2): 23-43.
- Galle, B., Johansson, M., Rivera, C., Zhang, Y., Kihlman, M., Kern, C., Lehmann, T., Platt, U., Arellano, S. and Hidalgo, S., 2010. Network for Observation of Volcanic and Atmospheric Change (NOVAC)&#8212;A global network for volcanic gas monitoring: Network layout and instrument description. *Journal of Geophysical Research*, 115(D05304): 1-19.
- Galle, B., Oppenheimer, C., Geyer, A., McGonigle, A.J.S., Edmonds, M. and Horrocks, L., 2003. A miniaturised ultraviolet spectrometer for remote sensing of SO<sub>2</sub> fluxes: a new tool for volcano surveillance. *Journal of Volcanology and Geothermal Research*, 119(1-4): 241-254.
- Hansell, A. and Oppenheimer, C., 2004. Health hazards from volcanic gases: a systematic literature review. *Archives of Environmental Health*, 59(12): 628-639.

- Ichoku, C. and Kaufman, Y.J., 2005. A method to derive smoke emission rates from MODIS fire radiative energy measurements. *IEEE Transactions on Geoscience and Remote Sensing*, 43(11): 2636-2649.
- Jarvis, A., Reuter, H.I., Nelson, A. and Guevara, E., 2008. Hole-filled SRTM for the globe Version 4. CGIAR-CSI SRTM 90m Database.
- Krotkov, N.A., Carn, S.A., Krueger, A.J., Bhartia, P.K. and Kai, Y., 2006. Band residual difference algorithm for retrieval of SO<sub>2</sub> from the aura ozone monitoring instrument (OMI). *IEEE Transactions on Geoscience and Remote Sensing*, 44(5): 1259-1266.
- Krueger, A.J., 1983. Sighting of El Chichón Sulfur Dioxide Clouds with the Nimbus 7 Total Ozone Mapping Spectrometer. *Science*, 220(4604): 1377-1379.
- Levelt, P.F., van den Oord, G.H.J., Dobber, M.R., Mälkki, A., Visser, H., de Vries, J., Stammes, P., Lundell, J.O.V. and Saari, H., 2006. The Ozone Monitoring Instrument. *IEEE Transactions on Geoscience and Remote Sensing*, 44(5): 1093-1101.
- Martini, F., Tassi, F., Vaselli, O., Del Potro, R., Martinez, M., Van del Laat, R. and Fernandez, E., 2010. Geophysical, geochemical and geodetical signals of reawakening at Turrialba volcano (Costa Rica) after almost 150 years of quiescence. *Journal of Volcanology and Geothermal Research*, 198(3-4): 416-432.
- McPeters, R.D., Bhartia, P.K., Krueger, A.J., Herman, J.R., Wellemeyer, C.G., Seftor, C.J., Jaross, G., Torres, O., Moy, L., Labow, G., Byerly, W., Taylor, S.L., Swissler, T. and Cebula, R.P., 1998. Earth Probe Total Ozone Mapping Spectrometer (TOMS) Data Products User's Guide. NASA Goddard Space Flight Center, Greenbelt, Maryland, pp. 1-70.
- Moffat, A.J. and Millan, M.M., 1971. The applications of optical correlation techniques to the remote sensing of SO<sub>2</sub> plumes using sky light. *Atmospheric Environment* (1967), 5(8): 677-690.
- OMI-Team, 2011. Ozone Monitoring Instrument (OMI) Data User's Guide. NASA. [http://disc.sci.gsfc.nasa.gov/Aura/additional/documentation/README.OMI\\_DUG.pdf](http://disc.sci.gsfc.nasa.gov/Aura/additional/documentation/README.OMI_DUG.pdf)
- Pinardi, G., Campion, R., Van Roozendaal, M., Fayt, C., Van Geffen, J., Galle, B., Carn, S.A., Valks, P., Rix, M., Hidalgo, S., Bourquin, J., Garzon, G., Inguaggiato, S. and Vita, F., 2010. Comparison of volcanic SO<sub>2</sub> flux measurements from satellite and from the NOVAC network, EUMETSAT Meteorological Satellite Conference. EUMETSAT, Cordoba, Spain, pp. 1-8.
- Reagan, M., Duarte, E., Soto, G.J. and Fernandez, E., 2006. The eruptive history of Turrialba volcano, Costa Rica, and potential hazards from future eruptions. In: W.I. Rose, G.J.S. Bluth, M.J. Carr, J.W. Ewert, L.C. Patino and J.W. Vallance (Editors), *Volcanic Hazards in Central America*. Geological Society of America, Boulder, CO, pp. 235-257.

- Resonance, L., 2007. Operational Manual Resonance Mini DOAS Spectrometer: Model # RMD-TCU, Ontario, Canada, pp. 1-21.
- Rolph, G.D., 2003. Real-time Environmental Applications and Display sYstem (READY) Website. NOAA Air Resources Laboratory, Silver Spring, MD.
- Shinohara, H., 2008. Excess degassing from volcanoes and its role on eruptive and intrusive activity. *Rev. Geophys.*, 46(4): RG4005.
- Simkin, T. and Siebert, L., 2002-2011a. Turrialba Eruptive History, Global Volcanism Program Digital Information Series. Smithsonian Institution.
- Simkin, T. and Siebert, L., 2002-2011b. Turrialba Weekly Reports, Global Volcanism Program Digital Information Series. Smithsonian Institution.
- Soto, G.J., 1988. Estructuras volcano-tectonicas del volcan Turrialba, Costa Rica, America Central, *Actas Quinto Congreso Geologico Chileno*, Santiago, Chile, pp. I 163-I 175.
- Soto, G.J., 2010. Preliminary Report Turrialba Volcano, Costa Rica: Current Activity January 4-10, 2010, National Seismological Network (RSN), San Jose, Costa Rica.
- Spinei, E., Carn, S.A., Krotkov, N.A., Mount, G.H., Yang, K. and Krueger, A.J., 2010. Validation of ozone monitoring instrument SO<sub>2</sub> measurements in the Okmok volcanic cloud over Pullman, WA, July 2008. *Journal of Geophysical Research*, 115(D00L08): 1-14.
- Stevenson, D.S., Johnson, C.E., Collins, W.J. and Derwent, R.G., 2003. The tropospheric sulphur cycle and the role of volcanic SO<sub>2</sub> In: C. Oppenheimer, D.M. Pyle and J. Barclay (Editors), *Volcanic Degassing*. Geological Society, Bath, UK, pp. 295-305.
- Stoiber, R.E. and Jepsen, A., 1973. Sulfur Dioxide Contributions to the Atmosphere by Volcanoes. *Science*, 182(4112): 577-578.
- Thomas, H. and Watson, I., 2010. Observations of volcanic emissions from space: current and future perspectives. *Natural Hazards*, 54(2): 323-354.
- Vandaele, A.C., Simon, P.C., Guilmot, J.M., Carleer, M. and Colin, R., 1994. SO<sub>2</sub> absorption cross section measurement in the UV using a Fourier transform spectrometer. *Journal of Geophysical Research*, 99(12): 25,599-525,605.
- Vaselli, O., Tassi, F., Duarte, E., Fernandez, E., Poreda, R.J. and Delgado, A., 2010. Evolution of fluid geochemistry at the Turrialba volcano (Costa Rica) from 1998 to 2008. *Bulletin of Volcanology*, 72(4): 397-410.
- Watson, I.M., Oppenheimer, C., Voight, B., Francis, P.W., Clarke, A., Stix, J., Miller, A., Pyle, D.M., Burton, M.R., Young, S.R., Norton, G., Loughlin, S. and Darroux, B., 2000. The relationship between degassing and ground deformation at Soufriere Hills Volcano, Montserrat. *Journal of Volcanology and Geothermal Research*, 98(1-4): 117-126.

- William-Jones, G., Stix, J. and Nadeau, P.A., 2008. Using the COSPEC in the Field. In: G. William-Jones, J. Stix and C. Hickson (Editors), The COSPEC Cookbook: Making SO<sub>2</sub> Measurements at Active Volcanoes. IAVCEI, pp. 63-119.
- Yang, K., Krotkov, N.A., Krueger, A.J., Carn, S.A., Bhartia, P.K. and Levelt, P.F., 2007. Retrieval of large volcanic SO<sub>2</sub> columns from the Aura Ozone Monitoring Instrument: Comparison and limitations. *Journal of Geophysical Research*, 112(D24S43): 1-14.
- Yang, K., Krotkov, N.A., Krueger, A.J., Carn, S.A., Bhartia, P.K. and Levelt, P.F., 2009. Improving retrieval of volcanic sulfur dioxide from backscattered UV satellite observations. *Geophysical Research Letters*, 36(L03102): 1-5.
- Young, S.R., Francis, P.W., Barclay, J., Casadevall, T.J., Gardner, C.A., Darroux, B., Davies, M.A., Delmelle, P., Norton, G.E., Maciejewski, A.J.H., Oppenheimer, C.M.M., Stix, J. and Watson, I.M., 1998. Monitoring SO<sub>2</sub> emission at the Soufriere Hills Volcano: Implications for changes in eruptive conditions. *Geophys. Res. Lett.*, 25(19): 3681-3684.

## 6. Appendix

### **A: Steps and parameters used to obtain data from NOAA's READY web-based system**

- 1) Navigate to the READY website: <http://ready.arl.noaa.gov/>
- 2) Choose the option “Archived Meteorology”
- 3) Input desired coordinates (Turrialba: 10.025,-83.767)
- 4) In the “Windrose” section, choose an archived dataset by clicking on the downward facing arrow and selecting the “GDAS (1 deg, 3 hourly, Global)”. Click Go.
- 5) Select the GDAS1 file for the period of interest by going to the section “GDAS1 Metereological File” and clicking on the downward facing arrow to select the desired date (data since December 1, 2004-present). Click Next.
- 6) Choose the day, hour (UTC), and wind rose duration for the analysis by clicking on the downward facing arrows and selecting the desired times.
- 7) In the “Level or averaged layer” section, click on the downward facing arrow on the “Level 1” subsection and select the desired pressure (mb) for the analysis which corresponds to the altitude of the wind data used for the analysis. Turrialba's volcanic plume is usually at ~3 km, where the pressure is ~700 mb.
- 8) Select the Output Options by clicking on them (Graphic and text, wind speed units in meters per second, wind rose size 96 dpi).
- 9) Type the access code displayed at the bottom right into the text box to retrieve the data. Click on Get Windrose.

10) A wind rose is computed using gridded model data, where you can click on the wind rose and save it as an image or you can obtain the text file by clicking on “Text Results” and save it.

## B: OMI monthly average SO<sub>2</sub> plots

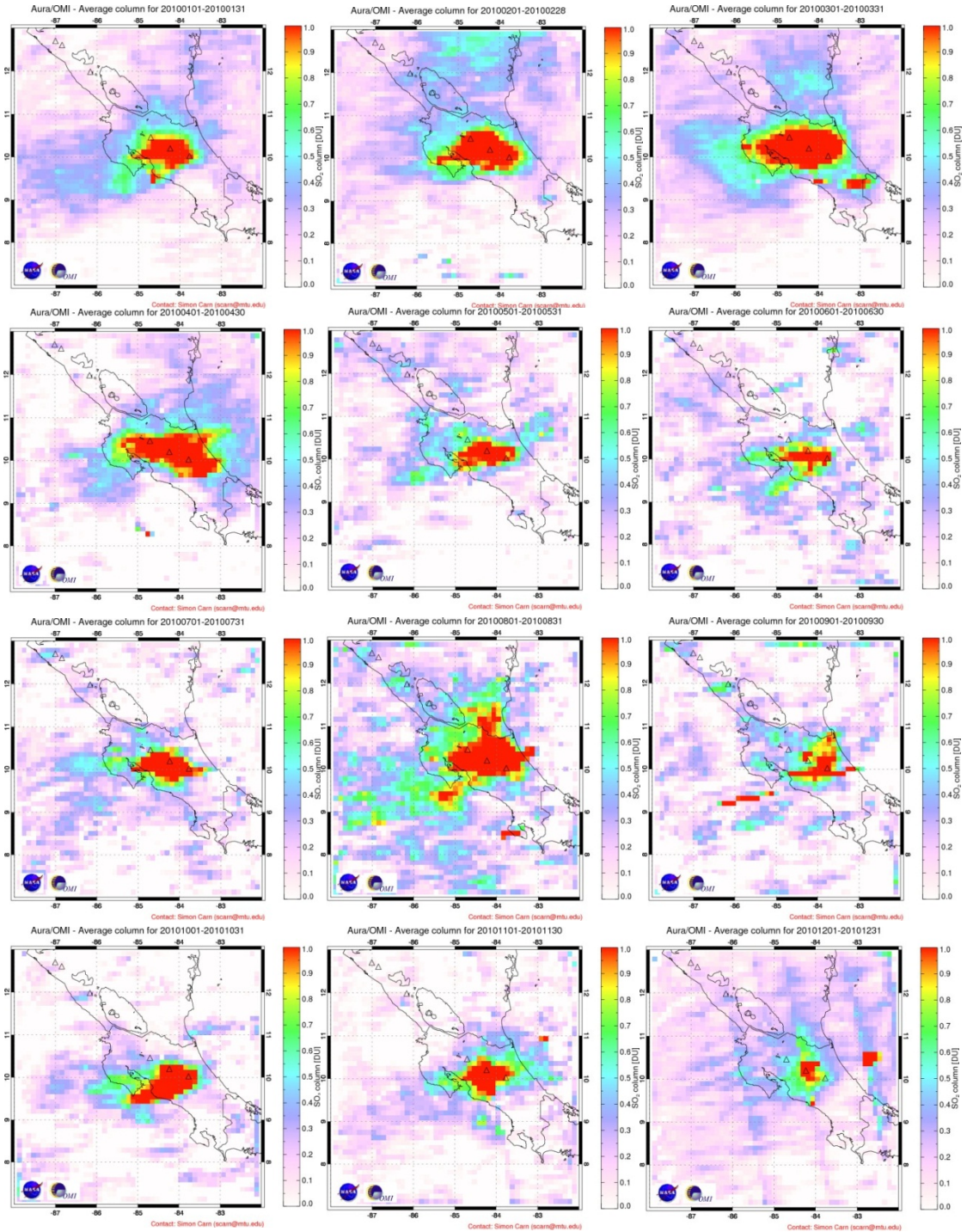


**Figure 21:** OMI monthly average SO<sub>2</sub> plots for the Costa Rica and Nicaragua region during 2010



## C: Processed NOVAC data

**Table 15:** NOVAC SO<sub>2</sub> fluxes (Galle et al., 2010), processed and provided by Vladimir Conde (personal communication, See Appendix G)

Date	Time (UTC)	SO <sub>2</sub> Flux (t/d)	Wind Speed (m/s)
4/23/2010	11:56	647.16	8.9
4/23/2010	12:29	3993.28	8.6
4/23/2010	12:40	3087.92	8.4
4/23/2010	12:56	3198.06	8.2
4/23/2010	13:15	3243.27	8.1
4/23/2010	13:22	3130.51	8.1
4/23/2010	13:31	4689.69	8.1
4/23/2010	13:40	4416.13	8.1
4/23/2010	13:48	3467.2	8
4/23/2010	13:56	3086.8	8
4/23/2010	14:03	2891.2	8
4/23/2010	14:09	4266.27	7.9
4/23/2010	14:15	3018.36	7.8
4/23/2010	14:21	3493.88	7.7
4/23/2010	14:29	3081.69	7.6
4/23/2010	14:35	3710.89	7.5
4/23/2010	14:40	3077.68	7.5
4/23/2010	14:46	3811.6	7.4
4/23/2010	14:51	2539.41	7.3
4/23/2010	14:56	3122.84	7.3
4/23/2010	15:02	3580.67	7.2
4/23/2010	15:09	3803.86	7.1
4/23/2010	15:14	3188.3	7
4/23/2010	15:21	3065.57	6.9
4/23/2010	15:26	2692.63	6.9
4/23/2010	15:41	3411.64	6.7
4/23/2010	15:51	3605.41	6.5
4/23/2010	15:56	2606.56	6.5
4/23/2010	16:01	2860.86	6.4
4/23/2010	16:05	3214.45	6.4
4/23/2010	16:11	3206.35	6.4
4/23/2010	16:15	2287.84	6.4
4/23/2010	16:19	2898.16	6.4
4/23/2010	16:24	2768.8	6.4
4/23/2010	16:29	2323.66	6.4
4/23/2010	16:33	1823.56	6.4

**Table 15, Continued**

<b>Date</b>	<b>Time (UTC)</b>	<b>SO<sub>2</sub> Flux (t/d)</b>	<b>Wind Speed (m/s)</b>
4/23/2010	16:37	1642.75	6.4
4/23/2010	16:41	809.87	6.4
4/23/2010	16:45	1676.28	6.4
4/23/2010	16:50	1395.06	6.4
4/23/2010	16:54	1478.07	6.4
4/23/2010	16:58	1806.68	6.4
4/23/2010	17:02	1670.7	6.4
4/23/2010	17:06	2137.99	6.3
4/23/2010	17:12	2113.73	6.2
4/23/2010	17:17	1886.23	6.1
4/23/2010	17:55	1152.02	5.6
4/23/2010	17:59	1193.61	5.5
4/23/2010	18:03	3038.23	5.5
4/23/2010	18:09	2586.95	5.4
4/23/2010	18:13	1486.94	5.4
4/23/2010	18:17	2465.16	5.4
4/23/2010	18:26	1547.65	5.3
4/23/2010	18:30	1452.51	5.2
4/23/2010	18:34	1587.73	5.2
4/23/2010	18:38	1062.28	5.2
4/23/2010	18:42	880.06	5.1
4/23/2010	18:46	890.09	5.1
4/23/2010	18:52	1148.03	5.1
4/23/2010	18:57	672.21	5
4/23/2010	19:06	1225.65	4.9
4/23/2010	19:11	835.43	4.8
4/28/2010	11:43	391.49	3.6
4/28/2010	12:00	273.14	3.3
4/28/2010	12:17	307.78	3
4/28/2010	12:45	242.15	2.5
4/28/2010	12:59	285.69	2.2
4/28/2010	13:30	324.83	2.5
4/28/2010	13:46	378.68	2.7
4/28/2010	14:01	380.35	2.8
4/28/2010	14:23	434	3.1
4/28/2010	14:54	601.04	3.4
4/28/2010	15:11	172.33	3.6
4/28/2010	15:27	845.86	3.8
4/28/2010	15:38	1709.25	3.9

**Table 15, Continued**

<b>Date</b>	<b>Time (UTC)</b>	<b>SO<sub>2</sub> Flux (t/d)</b>	<b>Wind Speed (m/s)</b>
4/28/2010	15:54	1121.5	4.1
4/28/2010	16:13	1045.48	4.1
4/28/2010	16:26	1055.16	4
4/28/2010	16:44	205.88	3.9
4/28/2010	16:56	1113.85	3.8
4/28/2010	17:13	480.24	3.9
4/28/2010	17:57	297.18	4.4
4/28/2010	18:17	953.13	4.2
4/28/2010	18:29	131.01	4.1
4/28/2010	18:42	365.94	4
4/28/2010	19:41	90.86	3.1
5/18/2010	12:13	703.12	4.1
5/18/2010	12:29	622.66	3.8
5/18/2010	12:59	687.51	3.1
5/18/2010	13:30	763.76	2.6
5/18/2010	13:47	565.08	2.4
5/18/2010	14:07	638.51	2.4
5/18/2010	14:20	593.46	2.6
5/18/2010	14:39	753.21	3
5/18/2010	14:51	774.77	3.3
5/18/2010	15:07	704.79	3.5
5/18/2010	15:24	1119.86	3.7
5/18/2010	16:03	404.57	3.9
5/18/2010	17:23	869.38	2.8
5/18/2010	17:56	472.31	2.5
5/18/2010	18:37	524.24	3.1
5/18/2010	18:46	1009.38	3.3
5/18/2010	19:21	931.58	3
5/30/2010	11:40	474.63	3.1
5/30/2010	11:56	512.31	2.5
5/30/2010	12:13	560.84	2.3
5/30/2010	12:28	564.29	2.1
5/30/2010	12:41	520.35	2
5/30/2010	12:50	530.13	1.9
5/30/2010	13:01	522.89	1.8
5/30/2010	13:09	490.58	1.6
5/30/2010	13:18	523.83	1.5
5/30/2010	13:28	495.43	1.3
5/30/2010	13:41	396.14	1

**Table 15, Continued**

<b>Date</b>	<b>Time (UTC)</b>	<b>SO<sub>2</sub> Flux (t/d)</b>	<b>Wind Speed (m/s)</b>
5/30/2010	13:53	273.21	0.8
5/30/2010	14:06	277.15	0.8
5/30/2010	14:17	287.54	0.9
5/30/2010	14:28	377.6	1.1
5/30/2010	14:37	384.2	1.2
5/30/2010	14:43	333.14	1.3
5/30/2010	14:53	331.33	1.4
5/30/2010	15:02	436.53	1.5
5/30/2010	15:12	364.6	1.5
5/30/2010	15:21	373.71	1.6
5/30/2010	15:30	372.8	1.6
5/30/2010	15:39	348.85	1.6
5/30/2010	15:47	444.92	1.7
5/30/2010	15:55	369.46	1.7
5/30/2010	16:03	416.75	1.7
5/30/2010	16:10	365.28	1.8
5/30/2010	16:16	326.62	1.8
5/30/2010	16:21	415.46	1.9
5/30/2010	16:26	482.6	1.9
5/30/2010	16:32	412.23	2
5/30/2010	16:37	661.09	2
5/30/2010	16:43	492.49	2.1
5/30/2010	16:48	390.43	2.1
5/30/2010	16:53	479.46	2.1
5/30/2010	16:58	603.75	2.2
5/30/2010	17:03	408.78	2.2
5/30/2010	17:09	331.58	2.2
5/30/2010	17:13	234.48	2.2
5/30/2010	17:17	170.83	2.2
5/30/2010	17:23	338.97	2.2
5/30/2010	17:27	172.2	2.2
5/30/2010	17:32	244.6	2.1
5/30/2010	17:36	272.58	2.1
5/30/2010	17:40	389.98	2.1
5/30/2010	17:44	432.07	2.1
5/30/2010	17:48	417.4	2.1
5/30/2010	17:52	288.69	2.1
5/30/2010	17:57	312.04	2.1
5/30/2010	18:03	27.09	2.1

**Table 15, Continued**

<b>Date</b>	<b>Time (UTC)</b>	<b>SO<sub>2</sub> Flux (t/d)</b>	<b>Wind Speed (m/s)</b>
5/30/2010	18:09	205.59	2.1
5/30/2010	18:14	189.75	2.1
5/30/2010	18:19	63.48	2
5/30/2010	18:25	65.13	2
5/30/2010	18:29	267.18	2
5/30/2010	18:42	34.72	2
5/30/2010	18:47	329.62	1.9
5/30/2010	18:52	220.53	1.9
5/30/2010	18:57	121.57	1.9
5/30/2010	19:02	197	1.9
5/30/2010	19:08	205.53	2
5/30/2010	19:12	117.57	2
5/30/2010	19:18	34.82	2.1
5/30/2010	19:23	28.54	2.1
5/30/2010	19:29	137.1	2.1
5/30/2010	19:34	328.53	2.2
6/10/2010	11:39	1120.98	5.2
6/10/2010	11:56	1158.87	4.8
6/10/2010	12:13	1031.11	4.4
6/10/2010	12:29	604.37	4
6/10/2010	12:46	580.88	3.6
6/10/2010	13:02	1086.52	3.2
6/10/2010	13:19	1109.72	3.2
6/10/2010	13:35	1315.57	3.2
6/10/2010	13:50	391.62	3.2
6/10/2010	14:07	276.83	3.1
6/10/2010	14:34	331.55	2.9
6/10/2010	15:08	530.92	2.6
6/10/2010	15:16	542.05	2.5
6/10/2010	15:25	475.44	2.5
6/10/2010	15:56	356.79	2.4
6/10/2010	16:57	1175.51	3.3
6/10/2010	17:11	945.36	3.2
6/10/2010	17:27	995.65	3.2
6/10/2010	17:49	126.14	3.1
6/10/2010	18:21	211.92	2.3
6/10/2010	18:39	126.92	1.8
6/10/2010	19:13	246.79	1.1
8/13/2010	12:13	466.58	2.2

---

**Table 15, Continued**

<b>Date</b>	<b>Time (UTC)</b>	<b>SO<sub>2</sub> Flux (t/d)</b>	<b>Wind Speed (m/s)</b>
8/13/2010	12:29	614.38	2.1
8/13/2010	12:46	384.3	2
8/13/2010	13:02	235.7	1.9
8/13/2010	13:19	263.34	1.9
8/13/2010	13:36	287.78	1.8
8/13/2010	13:52	331.14	1.8
8/13/2010	14:27	364.28	1.8
8/13/2010	14:48	632.84	1.9
8/13/2010	15:08	501.31	1.9

## D: MODIS smoke estimation technique

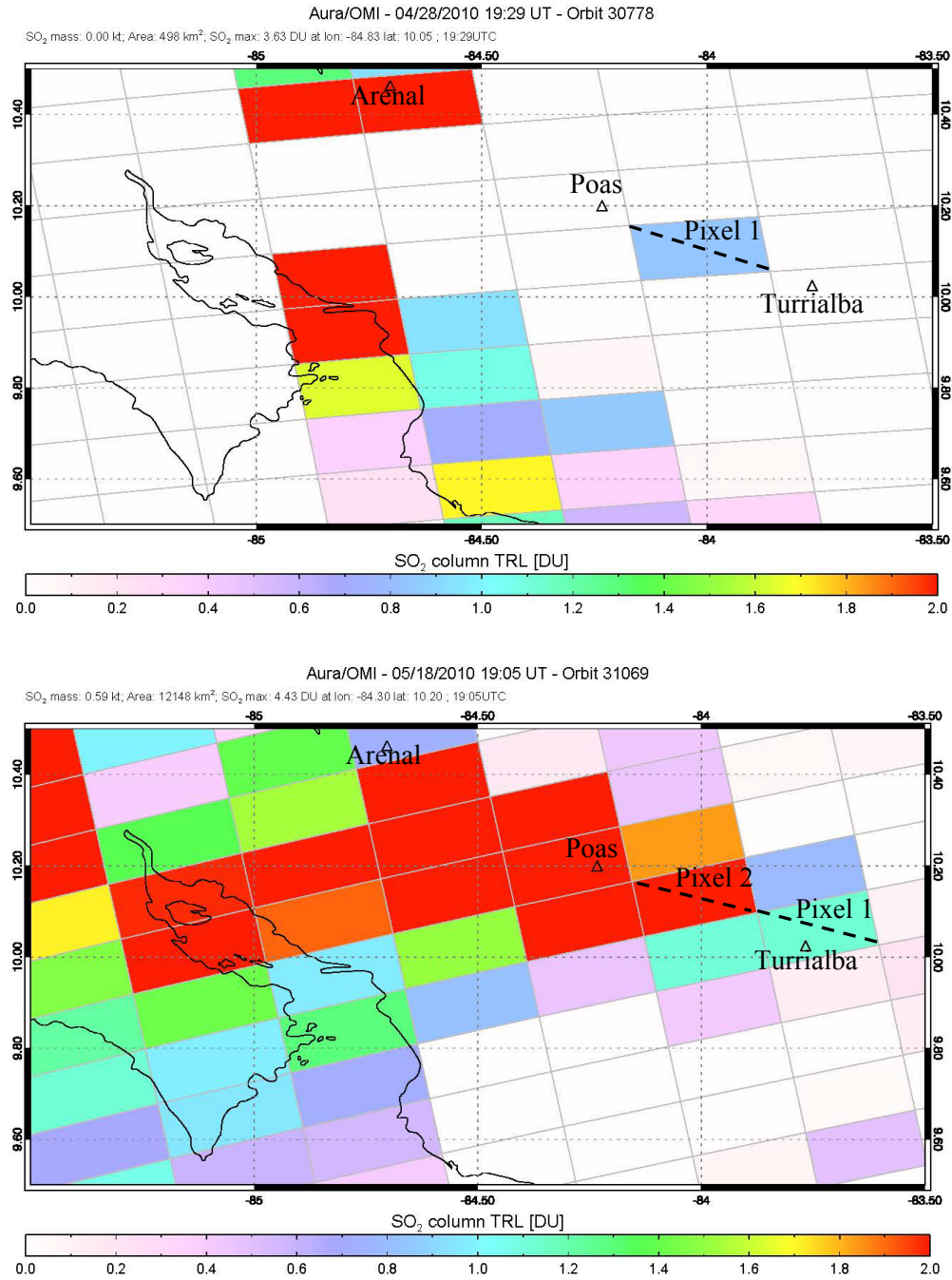


**Figure 22 A:** Pixels selected for OMI analysis using the MODIS smoke estimation technique for April 28, and May 18, 2010.

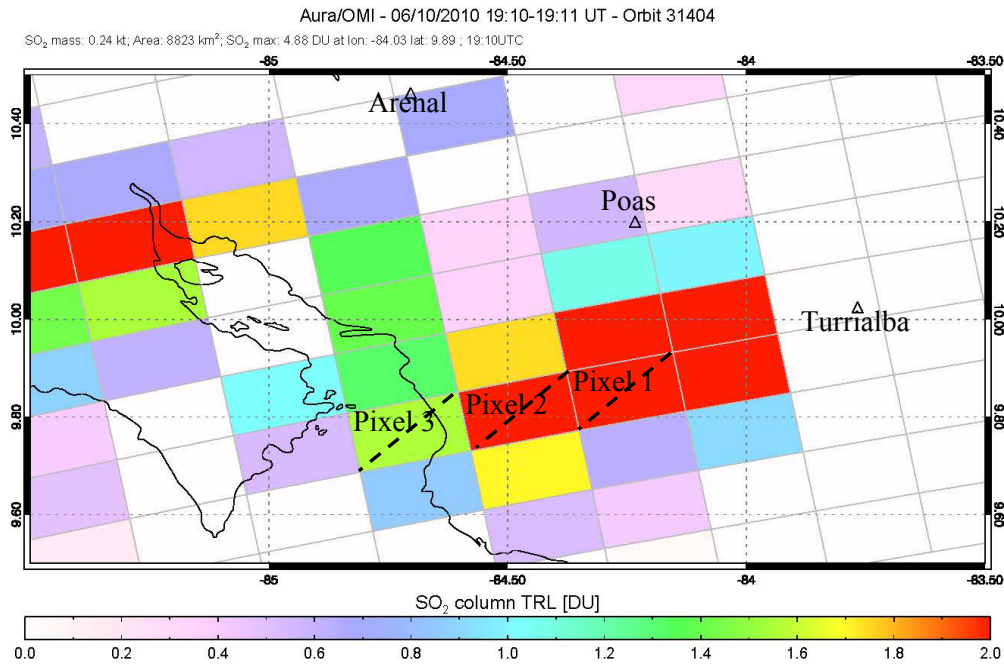
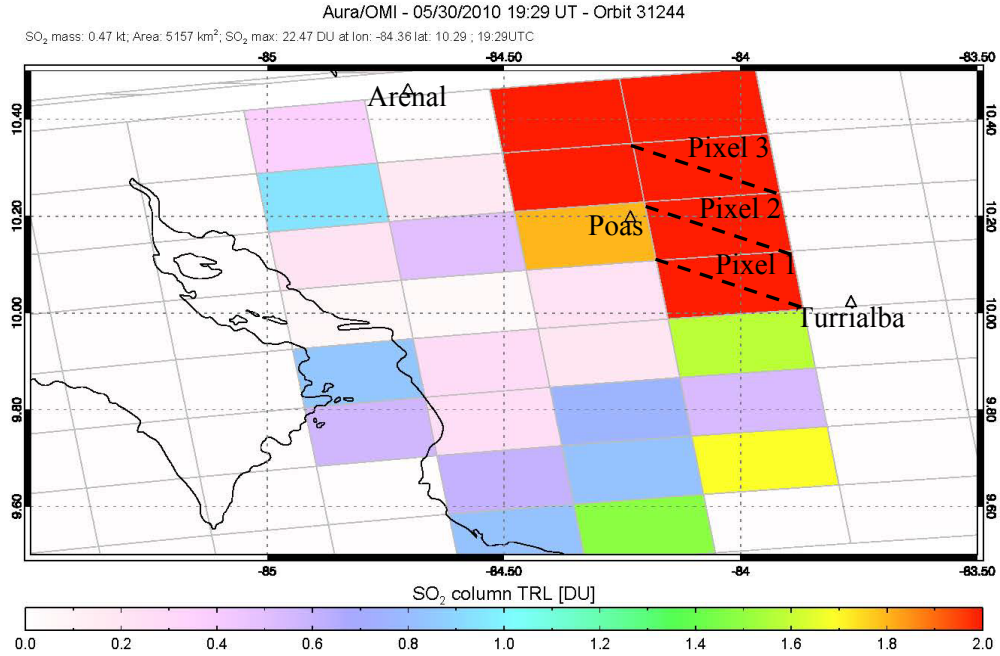


**Figure 22 B:** Pixels selected for OMI analysis using the MODIS smoke estimation technique for May 30, and June 10, 2010.



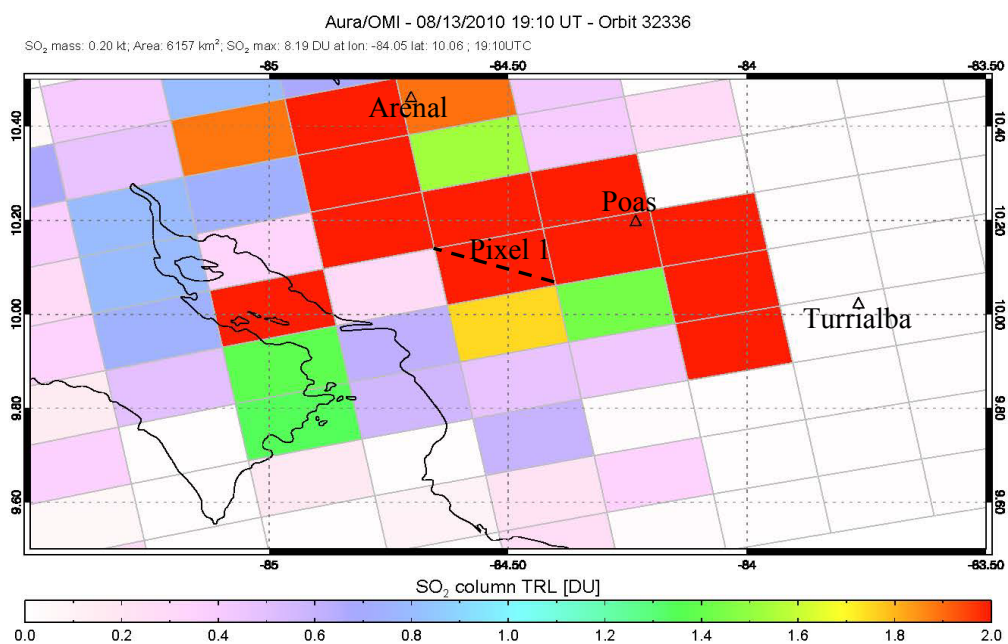


**Figure 22 C:** Pixels selected for OMI analysis using the MODIS smoke estimation technique for August 13, 2010.

## E: SO<sub>2</sub> transects from gridded OMI plots

4/23/2010

### Transect 1

Click mouse on 5KM SO<sub>2</sub> image to mark end points of traverse \*\*

-84.201804    9.9027712  
-84.206945    10.363364

Distance between two points (rhumb line) is: 51.276641 KM

Distance between two points (great circle) is: 51.276641 KM

Enter estimated windspeed (m/s): 6.4

PBL SO<sub>2</sub> flux (tons/day) = 3352.6309

TRL SO<sub>2</sub> flux (tons/day) = 888.21374

TRM SO<sub>2</sub> flux (tons/day) = 464.46060

STL SO<sub>2</sub> flux (tons/day) = 470.44756

### Transect 2

Click mouse on 5KM SO<sub>2</sub> image to mark end points of traverse \*\*

-84.320062    10.474616  
-84.320062    9.8977061

Distance between two points (rhumb line) is: 64.222022 KM

Distance between two points (great circle) is: 64.222022 KM

Enter estimated windspeed (m/s): 6.4

PBL SO<sub>2</sub> flux (tons/day) = 5937.2799

TRL SO<sub>2</sub> flux (tons/day) = 1310.6619

TRM SO<sub>2</sub> flux (tons/day) = 767.64128

STL SO<sub>2</sub> flux (tons/day) = 785.93471

### Transect 3

Click mouse on 5KM SO<sub>2</sub> image to mark end points of traverse \*\*

-84.433179    9.9027712  
-84.428038    10.474616

Distance between two points (rhumb line) is: 63.660663 KM

Distance between two points (great circle) is: 63.660663 KM

Enter estimated windspeed (m/s): 6.85

PBL SO<sub>2</sub> flux (tons/day) = 6618.3625

TRL SO<sub>2</sub> flux (tons/day) = 1621.3964

TRM SO<sub>2</sub> flux (tons/day) = 891.89951

STL SO<sub>2</sub> flux (tons/day) = 909.88843

### Transect 4

Click mouse on 5KM SO<sub>2</sub> image to mark end points of traverse \*\*

-84.546296    9.9027712  
-84.541155    10.474616

Distance between two points (rhumb line) is: 63.660663 KM

Distance between two points (great circle) is: 63.660663 KM

Enter estimated windspeed (m/s): 6.85  
PBL SO2 flux (tons/day) = 7551.1716  
TRL SO2 flux (tons/day) = 1999.9292  
TRM SO2 flux (tons/day) = 1041.2974  
STL SO2 flux (tons/day) = 1066.2291

#### Transect 5

Click mouse on 5KM SO2 image to mark end points of traverse \*\*

-84.664555 9.9027712  
-84.664555 10.469560

Distance between two points (rhumb line) is: 63.095329 KM

Distance between two points (great circle) is: 63.095329 KM

Enter estimated windspeed (m/s): 7.6

PBL SO2 flux (tons/day) = 7322.7531  
TRL SO2 flux (tons/day) = 1792.8607  
TRM SO2 flux (tons/day) = 987.78654  
STL SO2 flux (tons/day) = 1004.0848

#### Transect 6

Click mouse on 5KM SO2 image to mark end points of traverse \*\*

-84.777672 9.9027712  
-84.777672 10.358306

Distance between two points (rhumb line) is: 50.710503 KM

Distance between two points (great circle) is: 50.710503 KM

Enter estimated windspeed (m/s): 7.6

PBL SO2 flux (tons/day) = 4910.7140  
TRL SO2 flux (tons/day) = 1001.4643  
TRM SO2 flux (tons/day) = 673.85599  
STL SO2 flux (tons/day) = 663.59183

#### Transect 7

Click mouse on 5KM SO2 image to mark end points of traverse \*\*

-84.895930 9.9027712  
-84.890789 10.358306

Distance between two points (rhumb line) is: 50.713633 KM

Distance between two points (great circle) is: 50.713633 KM

Enter estimated windspeed (m/s): 8.066667

PBL SO2 flux (tons/day) = 4792.6711  
TRL SO2 flux (tons/day) = 1178.8362  
TRM SO2 flux (tons/day) = 692.13263  
STL SO2 flux (tons/day) = 640.09806

#### Transect 8

Click mouse on 5KM SO2 image to mark end points of traverse \*\*

-84.998764 9.9989935  
-84.998764 10.373480

Distance between two points (rhumb line) is: 41.688078 KM

Distance between two points (great circle) is: 41.688078 KM

Enter estimated windspeed (m/s): 8.066667

PBL SO2 flux (tons/day) = 4260.1439

TRL SO2 flux (tons/day) = 1358.1314

TRM SO2 flux (tons/day) = 634.60572

STL SO2 flux (tons/day) = 521.58289

#### Transect 9

Click mouse on 5KM SO2 image to mark end points of traverse \*\*

-85.070747 10.009120

-85.178723 10.358306

Distance between two points (rhumb line) is: 40.632063 KM

Distance between two points (great circle) is: 40.632063 KM

Enter estimated windspeed (m/s): 8.066667

PBL SO2 flux (tons/day) = 3861.8523

TRL SO2 flux (tons/day) = 1102.4452

TRM SO2 flux (tons/day) = 542.95401

STL SO2 flux (tons/day) = 448.35181

#### Transect 10

Click mouse on 5KM SO2 image to mark end points of traverse \*\*

-85.255848 10.252073

-85.147873 9.9078363

Distance between two points (rhumb line) is: 40.106428 KM

Distance between two points (great circle) is: 40.106428 KM

Enter estimated windspeed (m/s): 8.525

PBL SO2 flux (tons/day) = 4109.8323

TRL SO2 flux (tons/day) = 941.61691

TRM SO2 flux (tons/day) = 512.06440

STL SO2 flux (tons/day) = 435.04118

#### Transect 11

Click mouse on 5KM SO2 image to mark end points of traverse \*\*

-85.415240 10.125558

-85.070747 9.7913208

Distance between two points (rhumb line) is: 53.019539 KM

Distance between two points (great circle) is: 53.019537 KM

Enter estimated windspeed (m/s): 8.525

PBL SO2 flux (tons/day) = 3115.8170

TRL SO2 flux (tons/day) = 708.84284

TRM SO2 flux (tons/day) = 385.05080

STL SO2 flux (tons/day) = 341.37015

#### Transect 12

Click mouse on 5KM SO2 image to mark end points of traverse \*\*

-85.415240 10.009120

-85.189006 9.7862540

Distance between two points (rhumb line) is: 35.086146 KM  
Distance between two points (great circle) is: 35.086146 KM  
Enter estimated windspeed (m/s): 8.525  
PBL SO2 flux (tons/day) = 1584.9224  
TRL SO2 flux (tons/day) = 395.39943  
TRM SO2 flux (tons/day) = 214.25744  
STL SO2 flux (tons/day) = 190.16706

5/18/2010

#### Transect 1

Click mouse on 5KM SO2 image to mark end points of traverse \*\*

-83.811036 9.9432893  
-83.697919 10.160987

Distance between two points (rhumb line) is: 27.221965 KM  
Distance between two points (great circle) is: 27.221965 KM  
Enter estimated windspeed (m/s): 3  
PBL SO2 flux (tons/day) = 605.38968  
TRL SO2 flux (tons/day) = 151.50175  
TRM SO2 flux (tons/day) = 76.656399  
STL SO2 flux (tons/day) = 68.481540

#### Transect 2

Click mouse on 5KM SO2 image to mark end points of traverse \*\*

-83.872736 9.9432893  
-83.872736 10.272311

Distance between two points (rhumb line) is: 36.626895 KM  
Distance between two points (great circle) is: 36.626895 KM  
Enter estimated windspeed (m/s): 3.2  
PBL SO2 flux (tons/day) = 876.67576  
TRL SO2 flux (tons/day) = 321.88023  
TRM SO2 flux (tons/day) = 133.21369  
STL SO2 flux (tons/day) = 108.75970

#### Transect 3

Distance between two points (rhumb line) is: 49.045064 KM  
Distance between two points (great circle) is: 49.045064 KM  
Enter estimated windspeed (m/s): 2.65  
PBL SO2 flux (tons/day) = 762.06860  
TRL SO2 flux (tons/day) = 393.75283  
TRM SO2 flux (tons/day) = 146.56339  
STL SO2 flux (tons/day) = 112.66443

#### Transect 4

Click mouse on 5KM SO2 image to mark end points of traverse \*\*

-84.098970 9.9432893  
-84.098970 10.378537

Distance between two points (rhumb line) is: 48.452117 KM

Distance between two points (great circle) is: 48.452117 KM

Enter estimated windspeed (m/s): 3.9

PBL SO<sub>2</sub> flux (tons/day) = 1329.0835

TRL SO<sub>2</sub> flux (tons/day) = 665.85442

TRM SO<sub>2</sub> flux (tons/day) = 241.52293

STL SO<sub>2</sub> flux (tons/day) = 182.60874

#### Transect 5

Click mouse on 5KM SO<sub>2</sub> image to mark end points of traverse \*\*

-84.222371 9.9432893

-84.217229 10.383595

Distance between two points (rhumb line) is: 49.018361 KM

Distance between two points (great circle) is: 49.018361 KM

Enter estimated windspeed (m/s): 3.6

PBL SO<sub>2</sub> flux (tons/day) = 1938.9763

TRL SO<sub>2</sub> flux (tons/day) = 888.34693

TRM SO<sub>2</sub> flux (tons/day) = 298.27435

STL SO<sub>2</sub> flux (tons/day) = 250.02691

#### Transect 6

Click mouse on 5KM SO<sub>2</sub> image to mark end points of traverse \*\*

-84.340629 9.8318526

-84.330346 10.378537

Distance between two points (rhumb line) is: 60.867766 KM

Distance between two points (great circle) is: 60.867766 KM

Enter estimated windspeed (m/s): 2.825

PBL SO<sub>2</sub> flux (tons/day) = 1687.5547

TRL SO<sub>2</sub> flux (tons/day) = 692.33496

TRM SO<sub>2</sub> flux (tons/day) = 229.26141

STL SO<sub>2</sub> flux (tons/day) = 200.58898

#### Transect 7

Click mouse on 5KM SO<sub>2</sub> image to mark end points of traverse \*\*

-84.453746 9.8369187

-84.448604 10.484728

Distance between two points (rhumb line) is: 72.116776 KM

Distance between two points (great circle) is: 72.116776 KM

Enter estimated windspeed (m/s): 2.5

PBL SO<sub>2</sub> flux (tons/day) = 2015.1119

TRL SO<sub>2</sub> flux (tons/day) = 607.83167

TRM SO<sub>2</sub> flux (tons/day) = 267.99888

STL SO<sub>2</sub> flux (tons/day) = 255.60710

#### Transect 8

Click mouse on 5KM SO<sub>2</sub> image to mark end points of traverse \*\*

-84.572005 9.7254461

-84.551438 10.489784

Distance between two points (rhumb line) is: 85.116446 KM  
Distance between two points (great circle) is: 85.116446 KM  
Enter estimated windspeed (m/s): 3.666667  
PBL SO2 flux (tons/day) = 3762.6142  
TRL SO2 flux (tons/day) = 856.24697  
TRM SO2 flux (tons/day) = 484.02277  
STL SO2 flux (tons/day) = 481.73177

6/10/2010

#### Transect 1

Click mouse on 5KM SO2 image to mark end points of traverse \*\*

-84.042412 9.6494207  
-84.165812 10.216654

% Compiled module: MAP\_2POINTS.

Distance between two points (rhumb line) is: 64.578281 KM  
Distance between two points (great circle) is: 64.578281 KM  
Enter estimated windspeed (m/s): 3  
PBL SO2 flux (tons/day) = 1561.6778  
TRL SO2 flux (tons/day) = 776.81680  
TRM SO2 flux (tons/day) = 196.41660  
STL SO2 flux (tons/day) = 184.60062

#### Transect 2

Click mouse on 5KM SO2 image to mark end points of traverse \*\*

-84.170954 9.6443518  
-84.294354 10.221714

Distance between two points (rhumb line) is: 65.681253 KM  
Distance between two points (great circle) is: 65.681252 KM  
Enter estimated windspeed (m/s): 2.5  
PBL SO2 flux (tons/day) = 1443.7158  
TRL SO2 flux (tons/day) = 499.41092  
TRM SO2 flux (tons/day) = 183.36880  
STL SO2 flux (tons/day) = 181.21748

#### Transect 3

Click mouse on 5KM SO2 image to mark end points of traverse \*\*

-84.273787 9.6443518  
-84.412613 10.216654

Distance between two points (rhumb line) is: 65.502459 KM  
Distance between two points (great circle) is: 65.502459 KM  
Enter estimated windspeed (m/s): 3  
PBL SO2 flux (tons/day) = 2331.2791  
TRL SO2 flux (tons/day) = 747.09102  
TRM SO2 flux (tons/day) = 303.46406  
STL SO2 flux (tons/day) = 298.27837

#### Transect 4

Click mouse on 5KM SO2 image to mark end points of traverse \*\*

-84.392046    9.5328152  
-84.494879    10.105311

Distance between two points (rhumb line) is: 64.721166 KM

Distance between two points (great circle) is: 64.721166 KM

Enter estimated windspeed (m/s): 3.2

PBL SO2 flux (tons/day) = 2414.9443

TRL SO2 flux (tons/day) = 693.89254

TRM SO2 flux (tons/day) = 319.65498

STL SO2 flux (tons/day) = 307.85785

#### Transect 5

Click mouse on 5KM SO2 image to mark end points of traverse \*\*

-84.510304    9.5328152  
-84.607996    9.9888661

Distance between two points (rhumb line) is: 51.886889 KM

Distance between two points (great circle) is: 51.886889 KM

Enter estimated windspeed (m/s): 4

PBL SO2 flux (tons/day) = 2794.4935

TRL SO2 flux (tons/day) = 681.70335

TRM SO2 flux (tons/day) = 349.99179

STL SO2 flux (tons/day) = 329.61010

#### Transect 6

Click mouse on 5KM SO2 image to mark end points of traverse \*\*

-84.705688    9.6443518  
-84.643988    10.221714

Distance between two points (rhumb line) is: 64.627474 KM

Distance between two points (great circle) is: 64.627474 KM

Enter estimated windspeed (m/s): 5

PBL SO2 flux (tons/day) = 4166.8124

TRL SO2 flux (tons/day) = 855.29079

TRM SO2 flux (tons/day) = 515.47340

STL SO2 flux (tons/day) = 473.37019

7/23/2010

#### Transect 1

Click mouse on 5KM SO2 image to mark end points of traverse \*\*

-83.675533    10.290492  
-83.820735    9.8429454

Distance between two points (rhumb line) is: 52.301435 KM

Distance between two points (great circle) is: 52.301434 KM

Enter estimated windspeed (m/s): 5



PBL SO2 flux (tons/day) = 4544.8491  
TRL SO2 flux (tons/day) = 1212.0234  
TRM SO2 flux (tons/day) = 551.68112  
STL SO2 flux (tons/day) = 472.81778

#### Transect 2

Click mouse on 5KM SO2 image to mark end points of traverse \*\*

-83.946997 9.7371851  
-83.782856 10.278068

Distance between two points (rhumb line) is: 62.842805 KM

Distance between two points (great circle) is: 62.842804 KM

Enter estimated windspeed (m/s): 5

PBL SO2 flux (tons/day) = 6697.0558  
TRL SO2 flux (tons/day) = 1769.0059  
TRM SO2 flux (tons/day) = 818.26255  
STL SO2 flux (tons/day) = 704.18485

#### Transect 3

Click mouse on 5KM SO2 image to mark end points of traverse \*\*

-83.883866 10.284280  
-84.041694 9.7309628

Distance between two points (rhumb line) is: 63.979612 KM

Distance between two points (great circle) is: 63.979611 KM

Enter estimated windspeed (m/s): 5

PBL SO2 flux (tons/day) = 7638.3459  
TRL SO2 flux (tons/day) = 2020.4263  
TRM SO2 flux (tons/day) = 937.70515  
STL SO2 flux (tons/day) = 814.68533

#### Transect 4

Click mouse on 5KM SO2 image to mark end points of traverse \*\*

-83.984876 10.296703  
-84.111139 9.7309628

Distance between two points (rhumb line) is: 64.481724 KM

Distance between two points (great circle) is: 64.481724 KM

Enter estimated windspeed (m/s): 5

PBL SO2 flux (tons/day) = 7713.0594  
TRL SO2 flux (tons/day) = 2040.3102  
TRM SO2 flux (tons/day) = 952.85931  
STL SO2 flux (tons/day) = 839.14035

#### Transect 5

Click mouse on 5KM SO2 image to mark end points of traverse \*\*

-84.054320 10.389861  
-84.186896 9.7309628

Distance between two points (rhumb line) is: 74.774625 KM

Distance between two points (great circle) is: 74.774625 KM

Enter estimated windspeed (m/s): 5

PBL SO<sub>2</sub> flux (tons/day) = 8464.2526

TRL SO<sub>2</sub> flux (tons/day) = 2306.0108

TRM SO<sub>2</sub> flux (tons/day) = 1039.1013

STL SO<sub>2</sub> flux (tons/day) = 928.14023

#### Transect 6

Click mouse on 5KM SO<sub>2</sub> image to mark end points of traverse \*\*

-84.136391 10.389861

-84.281593 9.7309628

Distance between two points (rhumb line) is: 75.055854 KM

Distance between two points (great circle) is: 75.055853 KM

Enter estimated windspeed (m/s): 5

PBL SO<sub>2</sub> flux (tons/day) = 9099.5302

TRL SO<sub>2</sub> flux (tons/day) = 2584.3894

TRM SO<sub>2</sub> flux (tons/day) = 1110.9668

STL SO<sub>2</sub> flux (tons/day) = 1001.6318

#### Transect 7

Click mouse on 5KM SO<sub>2</sub> image to mark end points of traverse \*\*

-84.231088 10.389861

-84.369977 9.7371851

Distance between two points (rhumb line) is: 74.234068 KM

Distance between two points (great circle) is: 74.234068 KM

Enter estimated windspeed (m/s): 5

PBL SO<sub>2</sub> flux (tons/day) = 9515.0019

TRL SO<sub>2</sub> flux (tons/day) = 2765.9175

TRM SO<sub>2</sub> flux (tons/day) = 1152.1045

STL SO<sub>2</sub> flux (tons/day) = 1051.1982

#### Transect 8

Click mouse on 5KM SO<sub>2</sub> image to mark end points of traverse \*\*

-84.313159 10.389861

-84.458361 9.7371851

Distance between two points (rhumb line) is: 74.379054 KM

Distance between two points (great circle) is: 74.379053 KM

Enter estimated windspeed (m/s): 5

PBL SO<sub>2</sub> flux (tons/day) = 9414.7518

TRL SO<sub>2</sub> flux (tons/day) = 2744.7423

TRM SO<sub>2</sub> flux (tons/day) = 1142.2648

STL SO<sub>2</sub> flux (tons/day) = 1039.3428

#### Transect 9

Click mouse on 5KM SO<sub>2</sub> image to mark end points of traverse \*\*

-84.369977 10.489199

-84.546745    9.7434072

Distance between two points (rhumb line) is: 85.252203 KM

Distance between two points (great circle) is: 85.252202 KM

Enter estimated windspeed (m/s): 5

PBL SO2 flux (tons/day) = 9612.9292

TRL SO2 flux (tons/day) = 2824.4142

TRM SO2 flux (tons/day) = 1190.4169

STL SO2 flux (tons/day) = 1075.9760

Transect 10

Click mouse on 5KM SO2 image to mark end points of traverse \*\*

-84.458361    10.495407

-84.628815    9.7371851

Distance between two points (rhumb line) is: 86.448128 KM

Distance between two points (great circle) is: 86.448127 KM

Enter estimated windspeed (m/s): 5

PBL SO2 flux (tons/day) = 8637.6844

TRL SO2 flux (tons/day) = 2467.9342

TRM SO2 flux (tons/day) = 1074.9670

STL SO2 flux (tons/day) = 964.04518

Transect 11

Click mouse on 5KM SO2 image to mark end points of traverse \*\*

-84.641442    10.495407

-84.654068    9.7371851

Distance between two points (rhumb line) is: 84.417132 KM

Distance between two points (great circle) is: 84.417132 KM

Enter estimated windspeed (m/s): 5

PBL SO2 flux (tons/day) = 7439.9745

TRL SO2 flux (tons/day) = 2043.5951

TRM SO2 flux (tons/day) = 929.72402

STL SO2 flux (tons/day) = 823.36223

Transect 12

Click mouse on 5KM SO2 image to mark end points of traverse \*\*

-84.748765    10.495407

-84.748765    9.8429454

Distance between two points (rhumb line) is: 72.632481 KM

Distance between two points (great circle) is: 72.632481 KM

Enter estimated windspeed (m/s): 5

PBL SO2 flux (tons/day) = 6377.0657

TRL SO2 flux (tons/day) = 1697.3085

TRM SO2 flux (tons/day) = 808.89441

STL SO2 flux (tons/day) = 706.19622

Transect 13

Click mouse on 5KM SO2 image to mark end points of traverse \*\*

-84.856088 10.495407  
-84.856088 9.8429454

Distance between two points (rhumb line) is: 72.632481 KM

Distance between two points (great circle) is: 72.632481 KM

Enter estimated windspeed (m/s): 5

PBL SO2 flux (tons/day) = 6302.4386

TRL SO2 flux (tons/day) = 1640.6065

TRM SO2 flux (tons/day) = 812.17279

STL SO2 flux (tons/day) = 700.06203

Transect 14

Click mouse on 5KM SO2 image to mark end points of traverse \*\*

-84.982351 10.607122  
-84.976037 9.7434072

Distance between two points (rhumb line) is: 96.151809 KM

Distance between two points (great circle) is: 96.151809 KM

Enter estimated windspeed (m/s): 5

PBL SO2 flux (tons/day) = 7613.8562

TRL SO2 flux (tons/day) = 1990.6669

TRM SO2 flux (tons/day) = 1047.8038

STL SO2 flux (tons/day) = 887.84016

Transect 15

Click mouse on 5KM SO2 image to mark end points of traverse \*\*

-85.095987 10.607122  
-85.102300 9.7371851

Distance between two points (rhumb line) is: 96.844442 KM

Distance between two points (great circle) is: 96.844442 KM

Enter estimated windspeed (m/s): 5

PBL SO2 flux (tons/day) = 8618.9739

TRL SO2 flux (tons/day) = 2162.2394

TRM SO2 flux (tons/day) = 1193.5428

STL SO2 flux (tons/day) = 998.74344

Transect 16

Click mouse on 5KM SO2 image to mark end points of traverse \*\*

-85.203310 10.600917  
-85.209623 9.7247405

Distance between two points (rhumb line) is: 97.538986 KM

Distance between two points (great circle) is: 97.538986 KM

Enter estimated windspeed (m/s): 5

PBL SO2 flux (tons/day) = 9453.6150

TRL SO2 flux (tons/day) = 2301.9782

TRM SO2 flux (tons/day) = 1306.8870

STL SO2 flux (tons/day) = 1086.5402

01/28/2011

Transect 1

Click mouse on 5KM SO2 image to mark end points of traverse \*\*

-83.852300    10.054364  
-83.751290    9.5068855

Distance between two points (rhumb line) is: 61.944864 KM

Distance between two points (great circle) is: 61.944864 KM

Enter estimated windspeed (m/s): 8.5

PBL SO2 flux (tons/day) =    3240.5497

TRL SO2 flux (tons/day) =    1515.5941

TRM SO2 flux (tons/day) =    587.43319

STL SO2 flux (tons/day) =    354.03190

Transect 2

Click mouse on 5KM SO2 image to mark end points of traverse \*\*

-83.972250    10.048148  
-83.871240    9.5068855

Distance between two points (rhumb line) is: 61.264174 KM

Distance between two points (great circle) is: 61.264174 KM

Enter estimated windspeed (m/s): 8.5

PBL SO2 flux (tons/day) =    3761.3324

TRL SO2 flux (tons/day) =    1703.2638

TRM SO2 flux (tons/day) =    676.85036

STL SO2 flux (tons/day) =    400.20141

Transect 3

Click mouse on 5KM SO2 image to mark end points of traverse \*\*

-84.079573    10.147593  
-83.991189    9.5068855

Distance between two points (rhumb line) is: 71.979859 KM

Distance between two points (great circle) is: 71.979859 KM

Enter estimated windspeed (m/s): 8.5

PBL SO2 flux (tons/day) =    4378.0050

TRL SO2 flux (tons/day) =    2009.8173

TRM SO2 flux (tons/day) =    812.68235

STL SO2 flux (tons/day) =    476.96239

## **F: Copyright for Figure 12 (Personal communication through e-mail)**

Dear Anieri, At the figure caption they should include reproduced or modified with permission from IAVCEI

Cheers  
Adelina

-----  
Dr. Adelina Geyer Traver  
Institute of Earth Sciences "Jaume Almera" (CSIC)  
C/Lluís Solé i Sabarís s/n  
08028 Barcelona  
Spain  
office:+34 93 4095410

El 4/12/2011 11:09 PM, "Anieri M. Morales Rivera" <ammorale@mtu.edu> escribió:

Thanks Adelina!  
Looking forward to your reply

Anieri M. Morales Rivera

----- Original Message -----

From: "Adelina Geyer Traver" <ageyertraver@gmail.com>  
To: "Anieri M. Morales Rivera" <ammorale@mtu.edu>  
Sent: Friday, December 2, 2011 2:24:52 AM GMT -05:00 US/Canada Eastern  
Subject: Re: IAVCEI, Copyright, Figure for thesis  
Dear Anieri,  
I am checking it. I will keep you informed.  
Best regards, adelina

Dr. Adelina Geyer  
Institute of Earth Sciences Jaume Almera

El 30/11/2011 03:29, "Anieri M. Morales Rivera" <ammorale@mtu.edu> escribió:

Hello Adelina Geyer Traver,  
I am writing to you because I would like to use Figure 33 on Page 97  
From "The COSPEC Cookbook: Making SO<sub>2</sub> Gas Measurements at Active Volcanoes"  
(which was published online by IAVCEI) and include it in my thesis and I  
was wondering about the procedure I needed to follow in order to obtain a  
written statement saying that the Publisher (IAVCEI) gave me permission to  
use it. I would really appreciate your help!

Anieri M. Morales Rivera

## **G: Copyright for Appendix C (Personal communication through e-mail in Spanish)**

----- Original Message -----

From: "Vladimir Conde Jacobo" <conde@chalmers.se>

To: "Anieri M. Morales Rivera" <ammorale@mtu.edu>

Sent: Tuesday, October 18, 2011 2:58:11 PM GMT -05:00 US/Canada Eastern

Subject: RE: Emisiones Turrialba

Hola Anieri

La información meteorologica para los datos que te proporcioné fue tomada de 2 formas: la velocidad del viento viene de una estación

meteorologica: <http://www.imn.ac.cr/especial/estacionVturri.html>

La direccion de la pluma, la estimamos al medir los scans y determinar en que angulo se encuentra el centro de masa. Con ese angulo, las coordenadas del crater, de la estación y asumiendo una altura similar a la del crater; se triangula y se obtiene la direccion de la pluma.

Para el 2010 solo operó un instrumento, la estación se localiza en la finca silvia, y las coordenadas son:

lat=10.013526

long=-83.784457

alt=2676.434

Con respecto a las referencias,,,aun estoy trabajando en el paper, y espero tener el borrador en noviembre, si te urge referirlo, puedes hacerlo al proyecto NOVAC:

<http://www.agu.org/journals/jd/jd1005/2009JD011823/2009JD011823.pdf>

Si hay algo que aun no está claro no dudes en preguntarme

Saludos

A. Vladimir Conde

Phd. Student-Optical Remote Sensing Group

Chalmers University of Technology

Göteborg, Sweden

+46 (0)31-7721589

From: Anieri M. Morales Rivera [ammorale@mtu.edu]  
Sent: Tuesday, October 18, 2011 12:08 AM  
To: Vladimir Conde Jacobo  
Subject: Re: Emisiones Turrialba

Hola Vladimir,

Estaba viendo los datos otra vez y queria estar segura de que entendi correctamente: la informacion para estos datos en especificos son de la estacion metereologica en el volcan. De casualidad tienes las coordenadas de la estacion? Lo que decias de los modelos de viento te referias a otros volcanes en donde no tienen estaciones de viento instaladas? Estos datos son de un mismo instrumento, instrumentos diferentes, o de un valor promedio obtenido por los varios instrumentos que tienen instalados en el Turri? (Tienes las coordenadas del instrumento(s) que tomo las medidas?

Por otros temas, me podrias mandar cuando puedas la referencia de este trabajo ya sea un articulo publicado o un reporte/articulo no publicado o en revision?

Bueno, espero que te encuentres bien!

Anieri

----- Original Message -----

From: "Vladimir Conde Jacobo" <conde@chalmers.se>  
To: "Anieri M. Morales Rivera" <ammorale@mtu.edu>  
Sent: Thursday, September 22, 2011 5:56:01 PM GMT -05:00 US/Canada Eastern  
Subject: RE: Emisiones Turrialba

Hola

Estos datos asumen la pluma a la altura del crater, como te comenté es el año en que hubieron menos datos por problemas tecnicos, para enero solo tengo las mediciones del día en que fuimos con simon tarin y otros, no recuerdo que día fue ese, si te sirven, pues me dices.  
Aun no completo ni siquiera el draft de mi paper, para que puedas referir estos datos, pero creo que para cuando defiendas tu tesis, estaré mas avanzado espero

ok, en contacto

cuidate mucho

A. Vladimir Conde  
Phd. Student-Optical Remote Sensing Group



Chalmers University of Technology  
Göteborg, Sweden  
+46 (0)31-7721589

---

From: Anieri M. Morales Rivera [ammorale@mtu.edu]  
Sent: Thursday, September 22, 2011 11:08 PM  
To: Vladimir Conde Jacobo  
Subject: Emisiones Turrialba

Hola! Pues seria excelente si me pudieras proporcionar las emisiones procesadas de Turrialba dentro del año 2010. Ayer "jugando" con la base de datos trate de buscar data para el año 2010 completo y me salen demasiadas paginas de data (luego seguire tratando de entender esta base de datos). Trate tambien para enero del 2011 y especificamente para la semana despues de PASI (ultima semana de enero) pero no me dio ningun resultado. Me gustaria utilizar estas mediciones para compararla con mi data de OMI y con la de Simon Carn (quien es mi supervisor) durante el mismo periodo y posiblemente incluirla en mi tesis de maestria con tu permiso que planifico defender a finales de este semestre. Si quieres las proximas comunicaciones las hacemos en ingles para poder mandarselas tambien a Simon. Espero entonces tu contestacion. Aprecio muchisimo tu ayuda!

Anieri

----- Forwarded Message -----

From: "Anieri M. Morales Rivera" <ammorale@mtu.edu>  
To: "ammorale" <ammorale@mtu.edu>  
Sent: Thursday, September 22, 2011 10:45:44 AM GMT -05:00 US/Canada Eastern  
Subject: Vladimir

Mensaje de Vladimir

Hola Anieri

Que bueno saber de ti, pues mira he estado trabajando precisamente con los datos de NOVAC turrialba desde los inicios,,,para mala suerte en 2010 hay poco, solo unos meses estubo trabajando la estación, la reparé al terminar la reunión del PASI, y espero publicar mi paper para inicios del otro año.

Ahora, si entras a la basa de datos, en realidad lo que tienes son archivos comprimidos de espectros, para procesarlos necesitas el software NOVAC, a lo cual tienes que añadirle archivos de entrada que contienen informacions sobre la velocidad y dirección del viento, y la verdad no es tan facil, ese ha sido mi tarea de los ultimos meses con los volcanos en los que me he concentrado mas, y el mas importante para mi ahorita es turrialba.

Ahora si quieres te puedo proporcionar las emisiones que he procesado a partir de los espectros dentro del periodo 2010, pero como te comenté, son hay periodos largos en que no hubo mediciones....contactame a mi correo

conde@chalmers.se

estaré pendiente

saludos